Shape optimization of a thermoelastic body under thermal uncertainties

Marc Dambrine, Giulio Gargantini, Helmut Harbrecht, Viacheslav Karnaev

Shape optimization of a thermoelastic body under thermal uncertainties

Marc Dambrine[1], Giulio Gargantini[1], Helmut Harbrecht[2], and Viacheslav Karnaev[2]

[1]Universite de Pau et des Pays de l'Adour, E2S UPPA, CNRS, LMAP, Pau, France
[2]Departement Mathematik und Informatik, Universität Basel, Spiegelgasse 1, 4051 Basel, Switzerland

September 5, 2024

Abstract

We consider a shape optimization problem in the framework of the thermoelasticity model under uncertainty. The uncertainty is supposed to be located in the Robin boundary condition of the heat equation. The purpose of considering this model is to account for thermal residual stresses or thermal deformations, which may hinder the mechanical properties of the final design in case of a high environmental temperature. In this situation, the presence of uncertainty in the external temperature must be taken into account to ensure the correct manufacturing and performance of the device of interest. The objective functional under consideration is based on volume minimization in the presence of an inequality constraint for a quadratic shape functional. Exemplarily, we consider the L^2-norm of the von Mises stress and demonstrate that the robust constraint and its derivative are completely determined by low order moments of the random input, thus computable by means of low-rank approximation. The resulting shape optimization problem is discretized by using the finite element method for the underlying partial differential equations and the level-set method to represent the sought domain. Numerical results for a model case in structural optimization are given.

1 Introduction

If we consider the mechanical parts in a car, plane, or helicopter engine, they are subject to significant heat flows, high temperatures generated by the explosion of fuel or the evacuation of hot gases. Depending on the operating mode of the engine, these heat flows can vary significantly. Typically, they are higher when the engine is under heavy load, for example at start-up, and lower at idle. We aim to incorporate knowledge of this life cycle and its variability into the design of the structure. To do so, we want to

attack this problem through the prism of shape optimization by incorporating a priori known information about thermal loads to derive a volume shape that has a certain robustness to these loads. Consequently, our shape optimization problem must take into account two phenomena, mechanical and thermal, where we neglect the heat sources generated by the mechanical phenomena. It must take into account temporal effects and uncertainties about the temperature of the external environment.

Shape optimization under uncertainty is a topic of growing interest, see for example [1, 2, 6, 8, 10, 11, 12, 21] and the references therein. Less work has been done on shape optimization taking into account time evolution and thermoelasticity. We should mention the work [4] in the context of modeling residual stresses in additional manufacturing. Compared with these previous works, the main novelty of this article lays in the combination of the time dependency of the state and the objective with the account of uncertainties. Our main contribution is the expression of the shape derivatives for both, the time-averaged criterion and the value of the criterion at the final instant. We also demonstrate a two-dimensional configuration that our approach leads to effective calculations, where we see the importance and the impact of time-dependency and uncertainties on the environmental temperature.

The content of this article is as follows. In Section 2, our thermo-elastic evolution model is described in detail. The model consists of two partial differential equations, the time-dependent heat equation coupled to the quasi-static thermoelastic equation. Irreversible plastic deformations are neglected and not taken into account. We first define the model in the deterministic case assuming knowledge of the heat wave. Then, we present the shape optimization problem under consideration, namely the minimization of the volume of the structure under the constraint on the spatial L^2-norm of the von Mises stress. The constraint accounts for the thermoelastic model during the given time interval as well as the final state and depends on the applied thermal loading. Finally, we introduce the uncertainties on the applied thermal field which is seen as a given stochastic process. We consider the expectation of the objective and provide its deterministic expression by means of correlation operators.

From an application point of view, the L^∞-norm of von Mises stress would be of more interest. However, such a functional is not differentiable, so the L^p-norm is usually considered instead. To simplify further analysis, we restricted ourselves to the case $p = 2$. Nonetheless, the method presented in this article is not limited to this specific case but applies also to arbitrary p, see [7] for example.

Section 3 is the core of this article. It contains the shape calculus for the state equations and the respective shape functionals. Our main result is Theorem 3.8, providing effective formulae to compute the shape derivatives. The corresponding adjoint problems are introduced, allowing us to calculate the shape derivative of the constraint. In Section 4, we present the numerical setting and comment on the implementation. We perform numerical experiments in two spatial dimensions, validating our theoretical findings and showing the feasibility of the method. Finally, in Section 5, we state concluding remarks.

2 Problem formulation

We begin by introducing the necessary notation and defining the thermoelastic elasticity model, which consists of two systems of boundary values problems: one is the heat equation and one is the linear thermoelasticity system. A weak coupling is considered: while the effect of the temperature field on stresses is taken into account, the influence of mechanics on thermics is neglected. The elastic body is subjected to volume and surface loads. We assume that this body is placed in an external medium with which it exchanges heat. The heat exchange between the elastic body and the environment is modeled by the Robin boundary condition modeling the fact that the heat flux through the interface is proportional to the difference between their temperatures. We assume that the mechanical loads are known but that the temperature of the external environment varies significantly and randomly both in time and space. This section aims to establish a deterministic shape optimization problem constraint by a partial differential equation with random input.

2.1 Notation

First, we introduce some general notation. Let $D \subset \mathbb{R}^d,\ d = 2, 3$, be a bounded and connected domain with smooth boundary ∂D, which is divided into three subsets $\Gamma_{\mathcal{D}}$, $\Gamma_{\mathcal{N}}$ and $\Gamma_{\mathcal{F}}$ satisfying

$$|\Gamma_{\mathcal{D}}|, |\Gamma_{\mathcal{N}}|, |\Gamma_{\mathcal{F}}| > 0 \quad \text{such that} \quad \partial D = \Gamma_{\mathcal{D}} \cup \Gamma_{\mathcal{N}} \cup \Gamma_{\mathcal{F}}.$$

Hereinafter, we denote by $\boldsymbol{n}$ the outward pointing unit normal vector on ∂D.

We consider a thermoelastic body, represented by the region D, that undergoes heating and deformation over the time interval $(0, t_f)$. The state of the body is determined by the scalar field T of temperature and the vector field $\boldsymbol{u}$ of displacements:

$$T(t, \mathbf{x})\colon (0, t_f) \times D \to \mathbb{R}, \quad \boldsymbol{u}(t, \boldsymbol{x})\colon (0, t_f) \times D \to \mathbb{R}^d.$$

The properties of the body are completely characterized by the constant symmetric fourth-order stiffness tensor $\mathbb{C}$ and the matrix $\boldsymbol{B}$, which incorporate the material parameters: Young modulus $E > 0$, Poisson ratio $-1 < \nu < 1/2$, and the thermal expansion coefficient $\alpha > 0$.

Throughout the article, we use the following notation for the deformation tensor

$$\varepsilon(\boldsymbol{u}) := \frac{1}{2}(\boldsymbol{\nabla u} + \boldsymbol{\nabla u}^\top), \quad \text{where} \quad [\boldsymbol{\nabla u}]_{i,j} := \frac{\partial u_i}{\partial x_j}$$

and, according to the Duhamel-Neumann postulate, for the stress tensor

$$\sigma(\boldsymbol{u}, T) := \sigma_{\text{el}}(\boldsymbol{u}) + \sigma_{\text{th}}(T), \quad \sigma_{\text{el}}(\boldsymbol{u}) := \mathbb{C} : \varepsilon(\boldsymbol{u}), \quad \sigma_{\text{th}}(T) := (T - T_{\text{in}})\boldsymbol{B},$$

where

$$\mathbb{C} : \varepsilon(\boldsymbol{u}) = 2\mu\varepsilon(\boldsymbol{u}) + \lambda \operatorname{div}(\boldsymbol{u})\boldsymbol{I} \quad \text{and} \quad \boldsymbol{B} = -\alpha(3\lambda + 2\mu)\boldsymbol{I}.$$

Here, $\boldsymbol{I}$ is the identity matrix, $T_{\text{in}} \geq 0$ is the initial temperature and the Lamé constants are

$$\mu = \frac{E}{2(1+\nu)} \quad \text{and} \quad \lambda = \frac{E\nu}{(1+\nu)(1-2\nu)}.$$

Finally, we shall introduce the spaces of admissible solutions. To this end, we define the Sobolev space $H^1_{\mathcal{D}}(D) := \{u \in H^1(D) : u = 0 \text{ on } \Gamma_{\mathcal{D}}\}$ of H^1-smooth functions which vanish on $\Gamma_{\mathcal{D}}$ and set $H^{-1}(D) := \big(H^1_{\mathcal{D}}(D)\big)'$.

Let $(\Omega, \Sigma, \mathbb{P})$ be a complete probability space, and X and Y two Hilbert spaces. Then, the expectation of a random field $u \in L^2_{\mathbb{P}}[X]$ is given by

$$\mathbb{E}[u](x) = \int_\Omega u(x,\omega)\,\mathbb{P}(\mathrm{d}\omega) \in X,$$

while the two-point correlation function for two random fields $u \in L^2_{\mathbb{P}}[X]$ and $v \in L^2_{\mathbb{P}}[Y]$ is given by

$$\mathrm{Cor}[u,v](x,y) := \mathbb{E}[u \otimes v](x,y) = \int_\Omega u(x,\omega)v(y,\omega)\,\mathbb{P}(\mathrm{d}\omega) \in X \otimes Y.$$

2.2 Governing equations

We want to consider a model of the thermoelastic body D. First, we consider the deterministic case: the temperature $\widetilde{T}$ is assumed to be given and deterministic. To this end, we employ the heat equation and the equations of linear elasticity (see [25]). The mechanical unknowns of the model are the temperature field $T \in L^2((0,t_f); H^1(D)) \cap H^1\big((0,t_f); H^{-1}(D)\big)$ and the displacement field $\boldsymbol{u} \in L^2((0,t_f); H^1(D)^d)$, which are described by the following equations.

• **Heat equation.**

$$\begin{cases} \rho\dfrac{\partial T}{\partial t} - \mathrm{div}(k\nabla T) = Q \quad \text{in} \quad (0,t_f)\times D, \\ (k\nabla T)\cdot \boldsymbol{n} = -\beta(T-\widetilde{T}) \quad \text{on} \quad (0,t_f)\times \Gamma_{\mathcal{N}}\cup\Gamma_{\mathcal{F}}, \\ T = T_{\text{in}} \quad \text{on} \quad (0,t_f)\times\Gamma_{\mathcal{D}}, \\ T = T_{\text{in}} \quad \text{in} \quad \{t=0\}\times D. \end{cases} \tag{2.1}$$

Here, $\rho > 0$ is the product of the mass density by the specific heat capacity, $k > 0$ is the thermal conductivity coefficient, and $\beta > 0$ is the heat transfer coefficient. The thermal exchange with the environment is taken into account through the Robin boundary conditions with external temperature $\widetilde{T} \in L^2((0,t_f); L^2(\Gamma_{\mathcal{N}}\cup\Gamma_{\mathcal{F}}))$. Additionally, the body is influenced by a thermal body source $Q \in L^2((0,t_f); L^2(D))$.

- **Thermoelasticity equilibrium system.**

$$\begin{cases} -\operatorname{div}(\sigma(\boldsymbol{u},T)) = \boldsymbol{f} \ \text{ in } \ (0,t_f)\times D, \\ \sigma(\boldsymbol{u},T)\boldsymbol{n} = \boldsymbol{g} \ \text{ on } \ (0,t_f)\times \Gamma_{\mathcal{N}}, \\ \sigma(\boldsymbol{u},T)\boldsymbol{n} = \boldsymbol{0} \ \text{ on } \ (0,t_f)\times \Gamma_{\mathcal{F}}, \\ \boldsymbol{u} = \boldsymbol{0} \ \text{ on } \ (0,t_f)\times \Gamma_{\mathcal{D}}, \end{cases} \tag{2.2}$$

The thermoelastic body is subject to the body force $\boldsymbol{f} \in L^2((0,t_f);L^2(D)^d)$ in the whole domain D and to the surface force $\boldsymbol{g} \in L^2((0,t_f);L^2(\Gamma_{\mathcal{N}})^d)$ on the part $\Gamma_{\mathcal{N}}$ of the boundary. The body is assumed to be fixed on the part Γ_D of its boundary, while it is unconstrained on the rest $\Gamma_{\mathcal{F}}$ of the boundary. The illustration of the model can be found in the Figure 2.1.

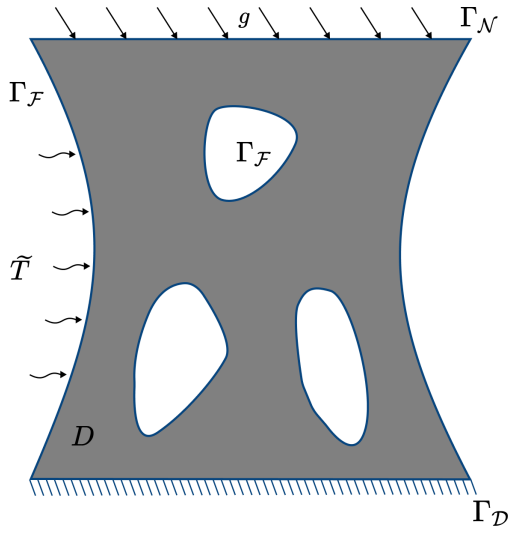

Figure 2.1: Illustration of the model for the thermoelastic body.

For the heat equation, we define the space $W((0,t_f),D)$ as

$$W((0,t_f),D) := \big\{T \in L^2((0,t_f);H^1(D)) \cap H^1((0,t_f);H^{-1}(D)) : \\ T = T_{\text{in}} \text{ on } (0,t_f)\times\Gamma_{\mathcal{D}} \text{ and } T = T_{\text{in}} \text{ in } \{t=0\}\times D\big\},$$

while, for the thermoelasticity equilibrium, we define the space $H((0,t_f),D)$ as $H((0,t_f),D) := L^2((0,t_f);H^1_{\mathcal{D}}(D)^d)$. Having these spaces at hand, the variational formulations associ-

ated to the problems (2.1) and (2.2) read as follows:

$$\begin{cases} \text{find } T \in W((0,t_f),D) \text{ such that for any } r \in L^2((0,t_f);H^1_{\mathcal{D}}(D)) \\ \displaystyle\int_0^{t_f}\int_D \rho\frac{\partial T}{\partial t} r \,\mathrm{d}\boldsymbol{x}\,\mathrm{d}t + \int_0^{t_f}\int_D k\nabla T\cdot\nabla r\,\mathrm{d}\boldsymbol{x}\,\mathrm{d}t + \int_0^{t_f}\int_{\Gamma_{\mathcal{N}}\cup\Gamma_{\mathcal{F}}} \beta T r\,\mathrm{d}\boldsymbol{s}\,\mathrm{d}t \\ \qquad = \displaystyle\int_0^{t_f}\int_D Q r\,\mathrm{d}\boldsymbol{x}\,\mathrm{d}t + \int_0^{t_f}\int_{\Gamma_{\mathcal{N}}\cup\Gamma_{\mathcal{F}}} \beta\widetilde{T} r\,\mathrm{d}\boldsymbol{s}\,\mathrm{d}t \end{cases} \tag{2.3}$$

and

$$\begin{cases} \text{find } \boldsymbol{u} \in H((0,t_f),D) \text{ such that for any } \boldsymbol{v} \in H((0,t_f),D) \\ \displaystyle\int_0^{t_f}\int_D \sigma_{\mathrm{el}}(\boldsymbol{u}) : \varepsilon(\boldsymbol{v})\,\mathrm{d}\boldsymbol{x}\,\mathrm{d}t = \int_0^{t_f}\int_D \boldsymbol{f}\cdot\boldsymbol{v}\,\mathrm{d}\boldsymbol{x}\,\mathrm{d}t + \int_0^{t_f}\int_{\Gamma_{\mathcal{N}}} \boldsymbol{g}\cdot\boldsymbol{v}\,\mathrm{d}\boldsymbol{x}\,\mathrm{d}t \\ \qquad\qquad - \displaystyle\int_0^{t_f}\int_D \sigma_{\mathrm{th}}(T) : \varepsilon(\boldsymbol{v})\,\mathrm{d}\boldsymbol{x}\,\mathrm{d}t. \end{cases} \tag{2.4}$$

It is well known, see [27], that (2.3) admits a unique solution $T \in W((0,t_f),D)$. Note that problem (2.3) can be solved independently of (2.4). Thus, $(T-T_{\mathrm{in}})\boldsymbol{B}$ becomes a forcing term in (2.4). Consequently, (2.4) also admits a unique solution $\boldsymbol{u} \in H((0,t_f),D)$.

2.3 Deterministic shape optimization problem

We are interested in the optimal shape of the body for the model described above. By optimal shape we mean the shape at which the objective functional reaches a minimum under the given constraints. In the present article, we consider two mechanical measures: the volume and the von Mises stress. The volume is defined as

$$\mathrm{Vol}(D) := \int_D \mathrm{d}\boldsymbol{x}$$

and the von Mises stress is defined as

$$\sigma_{\mathrm{VM}}(D) := \sqrt{\frac{d}{2}\sigma_d(\boldsymbol{u}_D) : \sigma_d(\boldsymbol{u}_D)},$$

where $\boldsymbol{u}_D$ is the solution of (2.2) in the domain D and σ_d is the stress deviator tensor

$$\sigma_d(\boldsymbol{u}) := \sigma(\boldsymbol{u},T) - \frac{\mathrm{tr}\,\sigma(\boldsymbol{u},T)}{d}\boldsymbol{I} = 2\mu\Big(\varepsilon(\boldsymbol{u}) - \frac{\mathrm{div}(\boldsymbol{u})}{d}\boldsymbol{I}\Big).$$

We shall next introduce the shape functional, which is the spatial L^2-norm of σ_{VM}, that is

$$\mathrm{VM}(D,t) := \frac{2}{d}\int_D |\sigma_{\mathrm{VM}}(\boldsymbol{u}_D(t,\boldsymbol{x}))|^2\,\mathrm{d}\boldsymbol{x} = \int_D \sigma_d(\boldsymbol{u}_D(t,\boldsymbol{x})) : \sigma_d(\boldsymbol{u}_D(t,\boldsymbol{x}))\,\mathrm{d}\boldsymbol{x}.$$

To address the time dimension, we introduce the parameters γ, $\delta \geq 0$ and consider a weighted combination of two options: $\mathrm{VM}(D,t)$ averaged in time and $\mathrm{VM}(D,t)$ taken at the final time, i.e.,

$$\mathrm{VM}_{\gamma,\delta}(D) := \gamma \int_0^{t_f} \mathrm{VM}(D,t)\ \mathrm{d}t + \delta\ \mathrm{VM}(D,t_f).$$

We are interested in the minimization of the volume $\mathrm{Vol}(D)$ of the body with a constraint on $\mathrm{VM}_{\gamma,\delta}(D)$ not to exceed a given threshold $\tau = \mathrm{const} > 0$. It is assumed that we are looking for an optimal structure D which is contained in some given bounded and connected reference domain D_{box} with smooth boundary. Thus, the problem is formulated as

$$\underset{D \subset D_{\mathrm{box}}}{\text{minimize}} \quad \mathrm{Vol}(D) \quad \text{subject to} \quad \mathrm{VM}_{\gamma,\delta}(D) \leq \tau. \tag{2.5}$$

For sake of simplicity, we consider the case when the boundaries $\Gamma_{\mathcal{D}}$ and $\Gamma_{\mathcal{N}}$ are non-optimizable, which is also reasonable from the application perspective.

Remark 2.1. *It should be noted that such a particular, but application-important shape optimization problem may not have a solution. We refer the reader to [3, Sct. 3.1] for an instructive example of non-existence of solutions. Even in cases where the shape optimization problem lacks a solution, there is still a significant practical value. Engineers frequently want to discover a component design that is better, but also close to the current one without necessarily achieving optimality.*

2.4 Adding uncertainties on the exterior temperature

In the next step, we want to consider the thermoelastic model (2.1) and (2.2) in the case when the external temperature in the Robin boundary condition is random. We take the external temperature as

$$\widetilde{T} \in L^2_{\mathbb{P}}[L^2((0,t_f); L^2(\Gamma_{\mathcal{N}} \cup \Gamma_{\mathcal{F}}))].$$

In turn, the displacement and temperature fields become also random: they are processes. By linearity of the systems and a priori estimates, one gets

$$T \in L^2_{\mathbb{P}}[W((0,t_f),D)] \text{ and } \boldsymbol{u} \in L^2_{\mathbb{P}}[H((0,t_f),D)].$$

Therefore, the functional $\mathrm{VM}(D,t,\omega)$ and, consequently, $\mathrm{VM}_{\gamma,\delta}(D,\omega)$ also depend on the random input field and become random processes.

In order to cast the shape optimization problem (2.5) into a deterministic one, we consider the expectation of $\mathrm{VM}_{\gamma,\delta}(D,\omega)$, which we denote by

$$J_{\gamma,\delta}(D) := \mathbb{E}[\mathrm{VM}_{\gamma,\delta}](D) = \gamma \int_0^{t_f} \mathbb{E}[\mathrm{VM}](D,t)\ \mathrm{d}t + \delta\, \mathbb{E}[\mathrm{VM}](D,t_f). \tag{2.6}$$

Consequently, in analogy to (2.5), the shape optimization problem under uncertainties reads

$$\underset{D \subset D_{\mathrm{box}}}{\text{minimize}} \quad \mathrm{Vol}(D) \quad \text{subject to} \quad J_{\gamma,\delta}(D) \leq \tau. \tag{2.7}$$

For sake of simplicity, we consider only the expected functional here, but its variance can also included as additional term, compare e.g. [11, 12].

Since the shape functionals in (2.7) are quadratic, we can express their expectation explicitly by means of the trace of the two-point correlation (see [9, Sct. 2] for the details).

Proposition 2.2. *Let us consider a functional $\mathcal{C}(\omega)$ in the form*

$$\mathcal{C}(\omega) = \langle \mathcal{B}\boldsymbol{u}(\omega), \boldsymbol{v}(\omega)\rangle = \mathcal{B} : (\boldsymbol{u}(\omega) \otimes \boldsymbol{v}(\omega)) \quad \textit{with} \quad \mathcal{B} : \mathbb{R}^{d^2} \to \mathbb{R}.$$

Then the expectation of $\mathcal{C}(\omega)$ can be expressed as

$$\mathbb{E}[\mathcal{C}] = \int_\Omega \mathcal{C}(\omega)\, \mathbb{P}(\mathrm{d}\omega) = \mathcal{B} : \mathrm{Cor}[\boldsymbol{u}, \boldsymbol{v}].$$

Since $\mathrm{VM}(D,t)$ is a quadratic functional, the expression for $\mathbb{E}[\mathrm{VM}](D,t)$ follows directly from Proposition 2.2.

Corollary 2.3. *There holds*

$$\mathbb{E}[\mathrm{VM}](D,t) = \int_D \big(\langle \sigma_d : \sigma_d \rangle \mathrm{Cor}[\boldsymbol{u}, \boldsymbol{u}]\big)((t,\boldsymbol{x}),(t',\boldsymbol{x}'))\big|_{(t',\boldsymbol{x}')=(t,\boldsymbol{x})}\, \mathrm{d}\boldsymbol{x},$$

where

$$\langle \sigma_d : \sigma_d \rangle : H((0,t_f),D) \otimes H((0,t_f),D) \to L^2((0,t_f)\times D) \otimes L^2((0,t_f)\times D)$$

is the linear operator induced by bilinear mapping $(\boldsymbol{u},\boldsymbol{v}) \to \sigma_d(\boldsymbol{u}) : \sigma_d(\boldsymbol{v})$.

With this result at hand, we immediately arrive at the following statement which can be used to compute the functional $J_{\gamma,\delta}(D,\omega)$ in accordance with (2.6).

Remark 2.4. *The two-point correlation $\mathrm{Cor}[\boldsymbol{u},\boldsymbol{u}]$ can be described by a tensor-product type boundary value problem. Such an expression is outside the scope of this article, thus we omit its formulation here. The interested reader is referred to [9], where this issue is discussed in detail.*

3 Shape calculus

Our next focus is the computation of the shape derivative of the functionals in the optimization problem (2.7) under consideration. We use the traditional method, in which the deformations of ∂D are parameterized by means of a vector field $\boldsymbol{\theta} \in W^{1,\infty}(D_{\mathrm{box}})^d$ and then the functionals are differentiated in the Fréchet sense with respect to $\boldsymbol{\theta}$. To this end, we introduce Lagrangian differentiation and calculate the derivatives of the temperature T and the displacement fields $\boldsymbol{u}$. Then, we compute the shape derivative of the functionals $\mathrm{Vol}(D)$ and $J_{\gamma,\delta}(D)$. For more details about shape calculus, we refer to [19, 26, 24].

3.1 Basic identities

First, we need to recall concept of shape differentiability. Let us consider a vector field $\boldsymbol{\theta} : D_{\text{box}} \to \mathbb{R}^d$ that belongs to $W^{1,\infty}(D_{\text{box}})^d$ such that

A1. the mapping $(\text{Id} + \boldsymbol{\theta})$ diffeomorphically takes the domain D_{box} on itself,

A2. there holds $\boldsymbol{\theta} = \mathbf{0}$ on $\Gamma_{\mathcal{D}} \cup \Gamma_{\mathcal{N}}$.

We define the family $D_{\boldsymbol{\theta}}$ of domains by setting $D_{\boldsymbol{\theta}} := (\text{Id} + \boldsymbol{\theta})(D)$.

To simplify the notation, we do not mention the random parameter, i.e., we always mean that $\widetilde{T}(\cdot,\cdot) \equiv \widetilde{T}(\cdot,\cdot,\omega)$, $T(\cdot,\cdot) \equiv T(\cdot,\cdot,\omega)$, and $\boldsymbol{u}(\cdot,\cdot) \equiv \boldsymbol{u}(\cdot,\cdot,\omega)$. We also want to focus on the fact that the displacement field and the temperature depend on the domain in which they are defined. For this purpose, we introduce the notation T_D and $\boldsymbol{u}_D$.

Next, we compute the derivatives of the temperature field T_D and displacement field $\boldsymbol{u}_D$ and in the *deterministic case*. We follow the Lagrangian approach and introduce the next definition.

Definition 3.1 (Lagrangian derivative)**.** *Let $D \subset \mathbb{R}^d$ be a bounded, Lipschitz domain and $\boldsymbol{u}_D : D \to \mathbb{R}^d$ be an associated function. The mapping $\boldsymbol{u}_D$ has a Lagrangian derivative at a particular shape D if the transported function*

$$\widehat{\boldsymbol{u}}_D(\boldsymbol{\theta}) := \boldsymbol{u}_{D_{\boldsymbol{\theta}}} \circ (\text{Id} + \boldsymbol{\theta})$$

is Fréchet differentiable at $\boldsymbol{\theta} = \mathbf{0}$. Its Fréchet derivative $\dot{\boldsymbol{u}}_D(\boldsymbol{\theta})$ is called the Lagrangian derivative of $\boldsymbol{u}_D$.

In the subsequent computations, we shall frequently use the surface divergence of a vector field, which is given by $\text{div}_{\boldsymbol{\tau}}(\boldsymbol{\theta}) = \text{div}(\boldsymbol{\theta}) - (\boldsymbol{\nabla\theta n}) \cdot \boldsymbol{n}$. Moreover, we introduce the following notation:

$$\begin{aligned} a(\boldsymbol{\theta}) &= \|(\boldsymbol{I} + \boldsymbol{\nabla\theta})^{-1}\boldsymbol{n}\| \,|\det(\boldsymbol{I} + \boldsymbol{\nabla\theta})|, \\ \boldsymbol{A}(\boldsymbol{\theta}) &= |\det(\boldsymbol{I} + \boldsymbol{\nabla\theta})|(\boldsymbol{I} + \boldsymbol{\nabla\theta})^{-1}(\boldsymbol{I} + \boldsymbol{\nabla\theta})^{-\top}, \\ \boldsymbol{A}'(\boldsymbol{\theta}) &= \text{div}(\boldsymbol{\theta})\boldsymbol{I} - \boldsymbol{\nabla\theta} - (\boldsymbol{\nabla\theta})^{\top}. \end{aligned} \tag{3.1}$$

With this notation at hand, we can formulate the following lemma which characterizes the Lagrangian derivative of the temperature field.

Lemma 3.2. *The Lagrangian derivative*

$$\dot{T}(t,\boldsymbol{x}) \in L^2((0,t_f); H^1_{\mathcal{D}}(D)) \cap H^1((0,t_f); H^{-1}(D))$$

of the solution of (2.1) *satisfies*

$$\begin{cases} \rho\dfrac{\partial \dot{T}}{\partial t} - \operatorname{div}(k\nabla \dot{T}) = \operatorname{div}(Q\boldsymbol{\theta}) - \rho\dfrac{\partial T}{\partial t} + \operatorname{div}(k\boldsymbol{A}'(\boldsymbol{\theta})\nabla T) \quad \textit{in} \quad (0,t_f)\times D, \\ (k\nabla \dot{T})\cdot \boldsymbol{n} + \beta \dot{T} = \operatorname{div}_{\boldsymbol{\tau}}(\beta \tilde{T}\boldsymbol{\theta}) - (k\boldsymbol{A}'(\boldsymbol{\theta})\nabla T)\cdot \boldsymbol{n} - \operatorname{div}_{\boldsymbol{\tau}}\boldsymbol{\theta}\beta T \quad \textit{on} \quad (0,t_f)\times \Gamma_{\mathcal{F}}, \\ (k\nabla \dot{T})\cdot \boldsymbol{n} = 0 \quad \textit{on} \quad (0,t_f)\times \Gamma_{\mathcal{N}}, \\ \dot{T} = 0 \quad \textit{on} \quad (0,t_f)\times \Gamma_{\mathcal{D}}, \\ \dot{T} = 0 \quad \textit{in} \quad \{t=0\}\times D. \end{cases} \tag{3.2}$$

Proof. First, we establish the variational formulation of (2.1) for the transported mapping $\widehat{T}_D(\boldsymbol{\theta}) = T_{D_{\boldsymbol{\theta}}} \circ (\mathrm{Id} + \boldsymbol{\theta})$. To achieve this, we start from the variational formulation (2.3) on the perturbed domain $D_{\boldsymbol{\theta}}$:

$$\begin{aligned} &\int_0^{t_f}\int_{D_{\boldsymbol{\theta}}} \rho\frac{\partial T_{D_{\boldsymbol{\theta}}}}{\partial t} r \,\mathrm{d}\boldsymbol{x}\,\mathrm{d}t + \int_0^{t_f}\int_{D_{\boldsymbol{\theta}}} k\nabla T_{D_{\boldsymbol{\theta}}}\cdot\nabla r \,\mathrm{d}\boldsymbol{x}\,\mathrm{d}t + \int_0^{t_f}\int_{\Gamma_{\mathcal{N}}\cup\Gamma_{\mathcal{F}\boldsymbol{\theta}}} \beta T_{D_{\boldsymbol{\theta}}} r \,\mathrm{d}\boldsymbol{s}\,\mathrm{d}t \\ &= \int_0^{t_f}\int_{D_{\boldsymbol{\theta}}} Q r \,\mathrm{d}\boldsymbol{x}\,\mathrm{d}t + \int_0^{t_f}\int_{\Gamma_{\mathcal{N}}\cup\Gamma_{\mathcal{F}\boldsymbol{\theta}}} \beta\widetilde{T} r \,\mathrm{d}\boldsymbol{s}\,\mathrm{d}t \quad \text{for any} \quad r\in L^2((0,t_f);H^1_{\mathcal{D}}(D)). \end{aligned}$$

Note that only the part $\Gamma_{\mathcal{F}}$ of the boundary is perturbed, since $\boldsymbol{\theta}=\mathbf{0}$ on $\Gamma_{\mathcal{D}}\cup\Gamma_{\mathcal{N}}$. We transport this formulation back to the original domain D by using the chain rule and a change of variables:

$$\begin{aligned} &\int_0^{t_f}\int_D \rho\frac{\partial \widehat{T}_D(\boldsymbol{\theta})}{\partial t} r|\det(\boldsymbol{I}+\boldsymbol{\nabla\theta})|\,\mathrm{d}\boldsymbol{x}\,\mathrm{d}t + \int_0^{t_f}\int_D k\boldsymbol{A}(\boldsymbol{\theta})\nabla\widehat{T}_D(\boldsymbol{\theta})\cdot\nabla r\,\mathrm{d}\boldsymbol{x}\,\mathrm{d}t \\ &+ \int_0^{t_f}\int_{\Gamma_{\mathcal{N}}\cup\Gamma_{\mathcal{F}}} \beta\widehat{T}_D(\boldsymbol{\theta}) r a(\boldsymbol{\theta})\,\mathrm{d}\boldsymbol{s}\,\mathrm{d}t = \int_0^{t_f}\int_D \widehat{Q}(\boldsymbol{\theta}) r|\det(\boldsymbol{I}+\boldsymbol{\nabla\theta})|\,\mathrm{d}\boldsymbol{x}\,\mathrm{d}t \\ &+ \int_0^{t_f}\int_{\Gamma_{\mathcal{N}}\cup\Gamma_{\mathcal{F}}} \beta\widehat{\widetilde{T}}(\boldsymbol{\theta}) r a(\boldsymbol{\theta})\,\mathrm{d}\boldsymbol{s}\,\mathrm{d}t \quad \text{for any} \quad r\in L^2((0,t_f);H^1_{\mathcal{D}}(D)). \end{aligned} \tag{3.3}$$

Here, the terms $\boldsymbol{A}(\boldsymbol{\theta})$ and $a(\boldsymbol{\theta})$ are defined in (3.1).

Next, we calculate the shape derivative of $\widehat{T}_D(\boldsymbol{\theta})$. The Fréchet differentiability of $\boldsymbol{\theta}\to\widehat{T}_D(\boldsymbol{\theta})$ follows from the implicit function theorem (see [19] for more details). We define $\mathcal{A}(\boldsymbol{\theta},\widehat{T}_D(\boldsymbol{\theta})) : W^{1,\infty}(D_{\mathrm{box}})^d \times W((0,t_f),D) \to L^2((0,t_f);H^{-1}(D))$ by

$$\begin{aligned} \mathcal{A}(\boldsymbol{\theta},\widehat{T}_D(\boldsymbol{\theta}))\langle r\rangle := &\int_0^{t_f}\int_D \rho\frac{\partial \widehat{T}_D(\boldsymbol{\theta})}{\partial t} r|\det(\boldsymbol{I}+\boldsymbol{\nabla\theta})|\,\mathrm{d}\boldsymbol{x}\,\mathrm{d}t \\ &+ \int_0^{t_f}\int_D k\boldsymbol{A}(\boldsymbol{\theta})\nabla\widehat{T}_D(\boldsymbol{\theta})\cdot\nabla r\,\mathrm{d}\boldsymbol{x}\,\mathrm{d}t + \int_0^{t_f}\int_{\Gamma_{\mathcal{N}}\cup\Gamma_{\mathcal{F}}} \beta\widehat{T}_D(\boldsymbol{\theta}) r a(\boldsymbol{\theta})\,\mathrm{d}\boldsymbol{s}\,\mathrm{d}t \end{aligned}$$

and $b(\boldsymbol{\theta}) : W^{1,\infty}(D_{\mathrm{box}})^d \to L^2((0,t_f);H^{-1}(D))$ by

$$b(\boldsymbol{\theta})\langle r\rangle := \int_0^{t_f}\int_D \widehat{Q}(\boldsymbol{\theta}) r|\det(\boldsymbol{I}+\boldsymbol{\nabla\theta})|\,\mathrm{d}\boldsymbol{x}\,\mathrm{d}t + \int_0^{t_f}\int_{\Gamma_{\mathcal{N}}\cup\Gamma_{\mathcal{F}}} \beta\widehat{\widetilde{T}}(\boldsymbol{\theta}) r a(\boldsymbol{\theta})\,\mathrm{d}\boldsymbol{s}\,\mathrm{d}t.$$

Thus, we can rewrite the identity (3.3) as

$$\mathcal{A}(\boldsymbol{\theta}, \widehat{T}_D(\boldsymbol{\theta})) = b(\boldsymbol{\theta}). \tag{3.4}$$

Taking the limit $\boldsymbol{\theta} \to \mathbf{0}$ yields

$$\mathcal{A}(\mathbf{0}, \dot{T}_D(\boldsymbol{\theta})) = b'(\mathbf{0})\langle\boldsymbol{\theta}\rangle - \mathcal{A}'(\mathbf{0}, T_D)\langle\boldsymbol{\theta}\rangle.$$

The involved derivatives have the following explicit expressions for arbitrary $\boldsymbol{\theta} \in W^{1,\infty}(D_{\mathrm{box}})^d$ with $\boldsymbol{\theta} = \mathbf{0}$ on $\Gamma_{\mathcal{D}} \cup \Gamma_{\mathcal{N}}$:

$$\begin{aligned}\mathcal{A}'(\mathbf{0}, T_D)\langle\boldsymbol{\theta}\rangle = &\int_0^{t_f}\int_D \operatorname{div}(\boldsymbol{\theta})\rho\frac{\partial T_D(\boldsymbol{\theta})}{\partial t} r \,\mathrm{d}\boldsymbol{x}\,\mathrm{d}t \\ &+ \int_0^{t_f}\int_D k\boldsymbol{A}'(\boldsymbol{\theta})\nabla T_D(\boldsymbol{\theta})\cdot\nabla r \,\mathrm{d}\boldsymbol{x}\,\mathrm{d}t + \int_0^{t_f}\int_{\Gamma_{\mathcal{F}}} \operatorname{div}_{\boldsymbol{\tau}}(\boldsymbol{\theta})\beta T_D r \,\mathrm{d}\boldsymbol{s}\,\mathrm{d}t.\end{aligned}$$

Here, $\boldsymbol{A}'(\boldsymbol{\theta}) = \operatorname{div}(\boldsymbol{\theta})\boldsymbol{I} - \boldsymbol{\nabla\theta} - (\boldsymbol{\nabla\theta})^\top$ and

$$b'(\mathbf{0})\langle\boldsymbol{\theta}\rangle = \int_0^{t_f}\int_D \operatorname{div}(Q\boldsymbol{\theta}) r \,\mathrm{d}\boldsymbol{x}\,\mathrm{d}t + \int_0^{t_f}\int_{\Gamma_{\mathcal{F}}} \operatorname{div}_{\boldsymbol{\tau}}(\beta\widetilde{T}\boldsymbol{\theta}) r \,\mathrm{d}\boldsymbol{s}\,\mathrm{d}t.$$

By combining the expressions above with (3.4), we conclude the variational identity

$$\begin{aligned}&\int_0^{t_f}\int_{D_{\boldsymbol{\theta}}} \rho\frac{\partial \dot{T}_D(\boldsymbol{\theta})}{\partial t} r \,\mathrm{d}\boldsymbol{x}\,\mathrm{d}t + \int_0^{t_f}\int_{D_{\boldsymbol{\theta}}} k\nabla\dot{T}_D(\boldsymbol{\theta})\cdot\nabla r \,\mathrm{d}\boldsymbol{x}\,\mathrm{d}t + \int_0^{t_f}\int_{\Gamma_{\mathcal{N}}\cup\Gamma_{\mathcal{F}\boldsymbol{\theta}}} \beta\dot{T}_D(\boldsymbol{\theta}) r \,\mathrm{d}\boldsymbol{s}\,\mathrm{d}t \\ &= \int_0^{t_f}\int_D \operatorname{div}(Q\boldsymbol{\theta}) r \,\mathrm{d}\boldsymbol{x}\,\mathrm{d}t + \int_0^{t_f}\int_{\Gamma_{\mathcal{F}}} \operatorname{div}_{\boldsymbol{\tau}}(\beta\widetilde{T}\boldsymbol{\theta}) r \,\mathrm{d}\boldsymbol{s}\,\mathrm{d}t - \int_0^{t_f}\int_D \operatorname{div}(\boldsymbol{\theta})\rho\frac{\partial T_D(\boldsymbol{\theta})}{\partial t} r \,\mathrm{d}\boldsymbol{x}\,\mathrm{d}t \\ &\qquad - \int_0^{t_f}\int_D k\boldsymbol{A}'(\boldsymbol{\theta})\nabla T_D(\boldsymbol{\theta})\cdot\nabla r \,\mathrm{d}\boldsymbol{x}\,\mathrm{d}t - \int_0^{t_f}\int_{\Gamma_{\mathcal{F}}} \operatorname{div}_{\boldsymbol{\tau}}(\boldsymbol{\theta})\beta T_D r \,\mathrm{d}\boldsymbol{s}\,\mathrm{d}t \\ &\qquad\qquad \text{for any} \quad r \in L^2((0,t_f); H^1(D)).\end{aligned} \tag{3.5}$$

Finally, the claim follows by applying Green's formula. □

The next lemma characterizes the Lagrangian derivative of the displacement field.

Lemma 3.3. *The Lagrangian derivative $\dot{\boldsymbol{u}}(t,\boldsymbol{x}) \in L^2((0,t_f); H^1_{\mathcal{D}}(D)^d)$ of the solution to (2.2) satisfies*

$$\begin{cases} -\operatorname{div}(\sigma_{\mathrm{el}}(\dot{\boldsymbol{u}})) = -\operatorname{div}\big((\mathbb{C}:\boldsymbol{\nabla u})\boldsymbol{\nabla\theta}^\top + \mathbb{C}:(\boldsymbol{\nabla\theta\nabla u}) - \operatorname{div}(\boldsymbol{\theta})\,\sigma(\boldsymbol{u},T) \\ \qquad\qquad - \boldsymbol{f}\otimes\boldsymbol{\theta} - \dot{T}\boldsymbol{B} + (T - T_{\mathrm{in}})\boldsymbol{B}\boldsymbol{\nabla\theta}^\top\big) \quad \text{in} \quad (0,t_f)\times D, \\ \sigma_{\mathrm{el}}(\dot{\boldsymbol{u}})\boldsymbol{n} = \big((\mathbb{C}:\boldsymbol{\nabla u})\boldsymbol{\nabla\theta}^\top + \mathbb{C}:(\boldsymbol{\nabla\theta\nabla u}) - \operatorname{div}(\boldsymbol{\theta})\sigma(\boldsymbol{u},T) \\ \qquad\qquad - \dot{T}\boldsymbol{B} + (T - T_{\mathrm{in}})\boldsymbol{B}\boldsymbol{\nabla\theta}^\top\big)\boldsymbol{n} \quad \text{on} \quad (0,t_f)\times\Gamma_{\mathcal{F}}, \\ \sigma_{\mathrm{el}}(\dot{\boldsymbol{u}})\boldsymbol{n} = \mathbf{0} \quad \text{on} \quad (0,t_f)\times\Gamma_{\mathcal{N}}, \\ \dot{\boldsymbol{u}} = \mathbf{0} \quad \text{on} \quad (0,t_f)\times\Gamma_{\mathcal{D}}. \end{cases} \tag{3.6}$$

Proof. The first step involves deriving a variational formulation for equation (2.2), which characterizes the transported mapping $\widehat{\boldsymbol{u}}D(\boldsymbol{\theta}) = \boldsymbol{u}_{D_{\boldsymbol{\theta}}} \circ (\mathrm{Id} + \boldsymbol{\theta})$. This is accomplished by applying the variational formulation presented in equation (2.4) within the perturbed domain $D_{\boldsymbol{\theta}}$:

$$\int_0^{t_f} \int_{D_{\boldsymbol{\theta}}} \sigma_{\mathrm{el}}(\boldsymbol{u}_{D_{\boldsymbol{\theta}}}) : \varepsilon(\boldsymbol{v}) \,\mathrm{d}\boldsymbol{x} \,\mathrm{d}t = \int_0^{t_f} \int_{D_{\boldsymbol{\theta}}} \boldsymbol{f} \cdot \boldsymbol{v} \,\mathrm{d}\boldsymbol{x} \,\mathrm{d}t + \int_0^{t_f} \int_{\Gamma_{\mathcal{N}}} \boldsymbol{g} \cdot \boldsymbol{v} \,\mathrm{d}\boldsymbol{x} \,\mathrm{d}t$$
$$- \int_0^{t_f} \int_{D_{\boldsymbol{\theta}}} \sigma_{\mathrm{th}}(T_{D_{\boldsymbol{\theta}}}) : \varepsilon(\boldsymbol{v}) \,\mathrm{d}\boldsymbol{x} \,\mathrm{d}t \quad \text{for any} \quad \boldsymbol{v} \in H((0,t_f), D_{\boldsymbol{\theta}}).$$

To revert to the original domain D, we employ the chain rule and a change of variables. Since $\boldsymbol{\theta} = \mathbf{0}$ on $\Gamma_{\mathcal{D}} \cup \Gamma_{\mathcal{N}}$, we obtain

$$\begin{aligned}
&\int_0^{t_f} \int_D \mathbb{C} : \boldsymbol{E}(\widehat{\boldsymbol{u}}_D(\boldsymbol{\theta}), \boldsymbol{\theta}) : \boldsymbol{E}(\boldsymbol{v}, \boldsymbol{\theta}) |\det(\boldsymbol{I} + \boldsymbol{\nabla}\boldsymbol{\theta})| \,\mathrm{d}\boldsymbol{x} \,\mathrm{d}t \\
&= \int_0^{t_f} \int_D \widehat{\boldsymbol{f}}(\boldsymbol{\theta}) \cdot \boldsymbol{v} |\det(\boldsymbol{I} + \boldsymbol{\nabla}\boldsymbol{\theta})| \,\mathrm{d}\boldsymbol{x} \,\mathrm{d}t + \int_0^{t_f} \int_{\Gamma_{\mathcal{N}}} \boldsymbol{g} \cdot \boldsymbol{v} \,\mathrm{d}\boldsymbol{s} \,\mathrm{d}t \\
&\quad - \int_0^{t_f} \int_D \sigma_{\mathrm{th}}(\widehat{T}_D(\boldsymbol{\theta})) : \boldsymbol{E}(\boldsymbol{v}) |\det(\boldsymbol{I} + \boldsymbol{\nabla}\boldsymbol{\theta})| \,\mathrm{d}\boldsymbol{x} \,\mathrm{d}t \quad \text{for any} \quad \boldsymbol{v} \in H((0,t_f), D),
\end{aligned} \tag{3.7}$$

where

$$\boldsymbol{E}(\boldsymbol{v}, \boldsymbol{\theta}) = \frac{1}{2}\Big((\boldsymbol{I} + \boldsymbol{\nabla}\boldsymbol{\theta})^{-1}\boldsymbol{\nabla}\boldsymbol{v} + \boldsymbol{\nabla}\boldsymbol{v}^{\top}(\boldsymbol{I} + \boldsymbol{\nabla}\boldsymbol{\theta})^{-\top}\Big).$$

Our aim is to compute the shape derivative of $\widehat{\mathbf{u}}_D(\boldsymbol{\theta})$. The Fréchet differentiability of $\boldsymbol{\theta} \to \widehat{\mathbf{u}}_D(\boldsymbol{\theta})$ is again a consequence of the implicit function theorem (see [19]). We define $\mathcal{A}(\boldsymbol{\theta}, \widehat{\boldsymbol{u}}_D(\boldsymbol{\theta})) : W^{1,\infty}(D_{\mathrm{box}})^d \times H((0,t_f), D) \to L^2((0,t_f); H^{-1}(D)^d)$ by

$$\mathcal{A}(\boldsymbol{\theta}, \widehat{\boldsymbol{u}}_D(\boldsymbol{\theta}))\langle \boldsymbol{v} \rangle := \int_0^{t_f} \int_D \mathbb{C} : \boldsymbol{E}(\widehat{\boldsymbol{u}}_D(\boldsymbol{\theta}), \boldsymbol{\theta}) : \boldsymbol{E}(\boldsymbol{v}, \boldsymbol{\theta}) |\det(\boldsymbol{I} + \boldsymbol{\nabla}\boldsymbol{\theta})| \,\mathrm{d}\boldsymbol{x} \,\mathrm{d}t$$

and $b(\boldsymbol{\theta}) : W^{1,\infty}(D_{\mathrm{box}})^d \to L^2((0,t_f); H^{-1}(D)^d)$ by

$$\begin{aligned}
b(\boldsymbol{\theta})\langle \boldsymbol{v} \rangle := &\int_0^{t_f} \int_D \widehat{\boldsymbol{f}}(\boldsymbol{\theta}) \cdot \boldsymbol{v} |\det(\boldsymbol{I} + \boldsymbol{\nabla}\boldsymbol{\theta})| \,\mathrm{d}\boldsymbol{x} \,\mathrm{d}t + \int_0^{t_f} \int_{\Gamma_{\mathcal{N}}} \boldsymbol{g} \cdot \boldsymbol{v} \,\mathrm{d}\boldsymbol{s} \,\mathrm{d}t \\
&- \int_0^{t_f} \int_D \sigma_{\mathrm{th}}(\widehat{T}_D(\boldsymbol{\theta})) : \boldsymbol{E}(\boldsymbol{v}) |\det(\boldsymbol{I} + \boldsymbol{\nabla}\boldsymbol{\theta})| \,\mathrm{d}\boldsymbol{x} \,\mathrm{d}t.
\end{aligned}$$

Hence, we can rewrite identity (3.7) as

$$\mathcal{A}(\boldsymbol{\theta}, \widehat{\boldsymbol{u}}_D(\boldsymbol{\theta})) = b(\boldsymbol{\theta}) \tag{3.8}$$

and taking the limit $\boldsymbol{\theta} \to \mathbf{0}$ implies

$$\mathcal{A}(\mathbf{0}, \dot{\boldsymbol{u}}_D(\boldsymbol{\theta})) = b'(\mathbf{0})\langle \boldsymbol{\theta} \rangle - \mathcal{A}'(\mathbf{0}, \boldsymbol{u}_D)\langle \boldsymbol{\theta} \rangle.$$

The derivatives can be explicitly characterized for any $\boldsymbol{\theta} \in W^{1,\infty}(D_{\text{box}})^d$ satisfying $\boldsymbol{\theta} = \mathbf{0}$ on $\Gamma_{\mathcal{D}} \cup \Gamma_{\mathcal{N}}$:

$$\mathcal{A}'(\mathbf{0}, T_D)\langle\boldsymbol{\theta}\rangle = \int_0^{t_f} \int_D \Big[\operatorname{div}(\boldsymbol{\theta})\sigma_{\text{el}}(\boldsymbol{u}_D) : \varepsilon(\boldsymbol{v}) \\ - \mathbb{C} : (\boldsymbol{\nabla\theta\nabla} \boldsymbol{u}_D) : \varepsilon(\boldsymbol{v}) - \mathbb{C} : \varepsilon(\boldsymbol{u}_D) : (\boldsymbol{\nabla\theta\nabla} \boldsymbol{v}) \Big] \,\mathrm{d}\boldsymbol{x}\,\mathrm{d}t$$

and

$$b'(\mathbf{0})\langle\boldsymbol{\theta}\rangle = \int_0^{t_f} \int_D \Big[\operatorname{div}(\boldsymbol{f} \otimes \boldsymbol{\theta}) \cdot \boldsymbol{v} - \dot{T}_D(\boldsymbol{\theta})\boldsymbol{B} : \varepsilon(\boldsymbol{v}) \\ + (T_D - T_{\text{in}})\boldsymbol{B}\boldsymbol{\nabla\theta}^\top : \boldsymbol{\nabla} \boldsymbol{v} - \operatorname{div}(\boldsymbol{\theta})\sigma_{\text{th}}(T_D) : \varepsilon(\boldsymbol{v}) \Big] \,\mathrm{d}\boldsymbol{x}\,\mathrm{d}t.$$

We combine these expressions with (3.8) and obtain the following variational identity:

$$\begin{aligned} &\int_0^{t_f} \int_D \sigma_{\text{el}}(\dot{\boldsymbol{u}}_D(\boldsymbol{\theta})) : \varepsilon(\boldsymbol{v}) \,\mathrm{d}\boldsymbol{x}\,\mathrm{d}t \\ &\qquad = \int_0^{t_f} \int_D \Big[\mathbb{C} : (\boldsymbol{\nabla\theta\nabla} \boldsymbol{u}_D) : \boldsymbol{\nabla} \boldsymbol{v} + \mathbb{C} : \boldsymbol{\nabla}(\boldsymbol{u}_D) : (\boldsymbol{\nabla\theta\nabla} \boldsymbol{v}) \\ &\qquad\qquad - \operatorname{div}(\boldsymbol{\theta})\sigma_{\text{el}}(\boldsymbol{u}_D) : \varepsilon(\boldsymbol{v}) + \operatorname{div}(\boldsymbol{f} \otimes \boldsymbol{\theta}) \cdot \boldsymbol{v} - \dot{T}\boldsymbol{B} : \varepsilon(\boldsymbol{v}) \\ &\qquad\qquad + (T - T_{\text{in}})\boldsymbol{B}\boldsymbol{\nabla\theta}^\top : \boldsymbol{\nabla} \boldsymbol{v} - \operatorname{div}(\boldsymbol{\theta})\sigma_{\text{th}}(T_D) : \varepsilon(\boldsymbol{v}) \Big] \,\mathrm{d}\boldsymbol{x}\,\mathrm{d}t. \end{aligned} \tag{3.9}$$

We finally prove the desired claim by applying Green's formula. □

3.2 Shape derivative

The objective of this subsection is the computation of the shape derivatives for the functionals of interest. The differentiability is defined in accordance with the following definition, compare [15, 19, 26].

Definition 3.4 (Fréchet differentiable shape functional)**.** *A shape functional $F(D)$ is Fréchet differentiable at D if there exists a linear continuous function $F'(D)\langle\cdot\rangle : W^{1,\infty}(D_{\text{box}})^d \to \mathbb{R}$ such that*

$$F(D_{\boldsymbol{\theta}}) = F(D) + F'(D)\langle\boldsymbol{\theta}\rangle + o(\boldsymbol{\theta})$$

for all $\boldsymbol{\theta} \in W^{1,\infty}(D_{\text{box}})^d$. The linear form $F'(D)\langle\cdot\rangle$ is called shape derivative of J in D.

In the context of unconstrained shape optimization, the shape derivative is employed to identify a direction $\boldsymbol{\theta}$ of deformation such that $F'(D)(\boldsymbol{\theta}) < 0$. This direction of deformation serves as a descent direction in a suitable optimization algorithm, allowing for the minimization of the objective functional $F(D)$. Before proceeding to the shape derivatives of the functionals, we need to mention an important theorem (see e.g. [19, 26] for a proof).

Theorem 3.5 (Hadamard's structure theorem)**.** *Let $D \in D_{\text{box}}$ be a C^1-smooth domain. We suppose that $F : D_{\text{box}} \to \mathbb{R}$ is a differentiable functional in the sense of Definition 3.4. If $\boldsymbol{\theta} \cdot \boldsymbol{n} = \mathbf{0}$ on the boundary ∂D, then $F'(D)\langle\boldsymbol{\theta}\rangle = 0$.*

The application of this theorem is explained in the following remark.

Remark 3.6. *In the case of sufficiently regular domain D, we can conclude from this theorem that the value of the derivative $F'(D)\langle\cdot\rangle$ depends only on the normal component of the vector field $\boldsymbol{\theta}$ on the boundary ∂D, i.e.*

$$F'(D) = \int_{\partial D} v_D(\boldsymbol{\theta} \cdot \boldsymbol{n}) \, \mathrm{d}\boldsymbol{s},$$

where $v_D : \partial D \to \mathbb{R}$ is a scalar field whose expression depends on the solutions of the underlying boundary value problems and the functional form. Thus, in the case of an unconstrained optimization problem, a descent direction $\boldsymbol{\theta}$ to the optimal shape is easily obtained by imposing that $\boldsymbol{\theta} = -v_D \boldsymbol{n}$ on ∂D. Consequently, we have

$$F'(D) = -\int_{\partial D} v_D^2 \, \mathrm{d}\boldsymbol{s} < 0.$$

We are now in the position to derive the shape derivatives of the functionals under consideration. The shape derivative of the volume of a body is not difficult to calculate, compare [26]. It is formulated in the following proposition.

Proposition 3.7. *The shape derivative of the volume* $\mathrm{Vol}(D)$ *is given by*

$$\mathrm{Vol}'(D)\langle\boldsymbol{\theta}\rangle = \int_{\Gamma_{\mathcal{F}}} (\boldsymbol{\theta} \cdot \boldsymbol{n}) \, \mathrm{d}\boldsymbol{s}. \tag{3.10}$$

The shape derivative of $J'_{\gamma,\delta}(D)\langle\boldsymbol{\theta}\rangle$ is presented in the next theorem.

Theorem 3.8. *The shape derivative of the $J_{\gamma,\delta}(D)$ is given by*

$$\begin{aligned}
J'_{\gamma,\delta}(D)\langle\boldsymbol{\theta}\rangle = {}& \\
& \gamma \int_0^{t_f} \int_{\Gamma_{\mathcal{F}}} \Big(\big(\langle\sigma_{\text{el}} : \varepsilon\rangle \mathrm{Cor}[\boldsymbol{u}_D, \boldsymbol{w}_D]\big)(t,\boldsymbol{x}) + \big(\langle\sigma_{\text{th}} : \varepsilon\rangle \mathrm{Cor}[T_D, \boldsymbol{w}_D]\big)(t,\boldsymbol{x}) \\
& \qquad + \big(\langle\sigma_d : \sigma_d\rangle \mathrm{Cor}[\boldsymbol{u}_D, \boldsymbol{u}_D]\big)(t,\boldsymbol{x}) + \boldsymbol{f}(t,\boldsymbol{x}) \cdot \mathbb{E}[\boldsymbol{w}_D](t,\boldsymbol{x}) \Big) (\boldsymbol{\theta} \cdot \boldsymbol{n}) \, \mathrm{d}\boldsymbol{x} \, \mathrm{d}t \\
& + \delta \int_{\Gamma_{\mathcal{F}}} \Big(\big(\langle\sigma_{\text{el}} : \varepsilon\rangle \mathrm{Cor}[\boldsymbol{u}_D, \boldsymbol{w}_D]\big)(t_f,\boldsymbol{x}) + \big(\langle\sigma_{\text{th}} : \varepsilon\rangle \mathrm{Cor}[T_D, \boldsymbol{w}_D]\big)(t_f,\boldsymbol{x}) \\
& \qquad + \big(\langle\sigma_d : \sigma_d\rangle \mathrm{Cor}[\boldsymbol{u}_D, \boldsymbol{u}_D]\big)(t_f,\boldsymbol{x}) + \boldsymbol{f}(t_f,\boldsymbol{x}) \cdot \mathbb{E}[\boldsymbol{w}_D](t_f,\boldsymbol{x}) \Big) (\boldsymbol{\theta} \cdot \boldsymbol{n}) \, \mathrm{d}\boldsymbol{x} \\
& + \int_0^{t_f} \int_{\Gamma_{\mathcal{F}}} \Big(\beta \Big(\mathcal{H} - \frac{2\beta}{k} \Big) \mathrm{Cor}[\widetilde{T} - T_D, p_D](t,\boldsymbol{x}) - \beta \mathrm{Cor}[\partial \widetilde{T}/\partial \boldsymbol{n}, p_D](t,\boldsymbol{x}) \\
& \qquad + Q(t,\boldsymbol{x}) \mathbb{E}[p_D](t,\boldsymbol{x}) - \rho \, \mathrm{Cor}[\partial T_D/\partial t, p_D](t,\boldsymbol{x}) \\
& \qquad - k \big(\langle\nabla \otimes \nabla\rangle \mathrm{Cor}[T_D, p_D]\big)(t,\boldsymbol{x}) \Big) (\boldsymbol{\theta} \cdot \boldsymbol{n}) \, \mathrm{d}\boldsymbol{x} \, \mathrm{d}t,
\end{aligned} \tag{3.11}$$

where $T_D \in L^2_{\mathbb{P}}[\Omega; W((0,t_f),D)]$ *is the solution of* (2.1) *with the Robin boundary data* $\widetilde{T} \in L^2_{\mathbb{P}}[\Omega; L^2((0,t_f); L^2(\Gamma_{\mathcal{N}} \cup \Gamma_{\mathcal{F}}))]$ *and* $\boldsymbol{u}_D \in L^2_{\mathbb{P}}[\Omega; H((0,t_f),D)]$ *is the associated solution of* (2.2)*. The function* $\boldsymbol{w}_D \in L^2_{\mathbb{P}}[\Omega; H((0,t_f),D)]$ *satisfies the following adjoint system*

$$\begin{cases} -\operatorname{div}(\sigma_{\mathrm{el}}(\boldsymbol{w}_D)) = 4\mu \operatorname{div}(\sigma_d(\boldsymbol{u}_D)) \quad \textit{in} \quad (0,t_f)\times D, \\ \sigma_{\mathrm{el}}(\boldsymbol{w}_D)\boldsymbol{n} = 4\mu\sigma_d(\boldsymbol{u}_D)\boldsymbol{n} + \boldsymbol{g} \quad \textit{on} \quad (0,t_f)\times \Gamma_{\mathcal{N}}, \\ \sigma_{\mathrm{el}}(\boldsymbol{w}_D)\boldsymbol{n} = 4\mu\sigma_d(\boldsymbol{u}_D)\boldsymbol{n} \quad \textit{on} \quad (0,t_f)\times \Gamma_{\mathcal{F}}, \\ \boldsymbol{w} = \boldsymbol{0} \quad \textit{on} \quad (0,t_f)\times \Gamma_{\mathcal{D}}, \end{cases} \tag{3.12}$$

while $p_D \in L^2_{\mathbb{P}}[\Omega; P_\delta((0,t_f),D)]$ *satisfies another backward in time adjoint system*

$$\begin{cases} \rho\dfrac{\partial p_D}{\partial t} + \operatorname{div}(k\nabla p_D) = -\gamma \boldsymbol{B} : \boldsymbol{\nabla w}_D \quad \textit{in} \quad (0,t_f)\times D, \\ (k\nabla p_D)\cdot \boldsymbol{n} + \beta p_D = 0 \quad \textit{on} \quad (0,t_f)\times \Gamma_{\mathcal{N}} \cup \Gamma_{\mathcal{F}}, \\ p_D = 0 \quad \textit{on} \quad (0,t_f)\times \Gamma_{\mathcal{D}}, \\ p_D = \delta \boldsymbol{B} : \boldsymbol{\nabla w}_D \quad \textit{in} \quad \{t=t_f\}\times D. \end{cases} \tag{3.13}$$

Here, the function space $P_\delta((0,t_f),D)$ *is defined as*

$$\begin{aligned} P_\delta((0,t_f),D) := \big\{ & p_D \in L^2((0,t_f); H^1(D)) \cap H^1((0,t_f); H^{-1}_{\mathcal{D}}(D)) : \\ & p_D = 0 \text{ on } (0,t_f)\times\Gamma_{\mathcal{D}} \text{ and } p_D = \delta \boldsymbol{B} : \boldsymbol{\nabla w}_D \text{ in } \{t=t_f\}\times D \big\} \end{aligned}$$

and the linear operators

$$\begin{aligned} \langle \nabla\otimes\nabla\rangle &: W((0,t_f),D)\otimes P_\delta((0,t_f),D) \to L^2((0,t_f)\times D)\otimes L^2((0,t_f)\times D), \\ \langle \sigma_{\mathrm{el}} : \varepsilon\rangle &: H((0,t_f),D)\otimes H((0,t_f),D) \to L^2((0,t_f)\times D)\otimes L^2((0,t_f)\times D), \\ \langle \sigma_{\mathrm{th}} : \varepsilon\rangle &: W((0,t_f),D)\otimes H((0,t_f),D) \to L^2((0,t_f)\times D)\otimes L^2((0,t_f)\times D), \end{aligned}$$

are induced by the bilinears mappings

$$(T,p) \to \nabla T\cdot\nabla p, \quad (\boldsymbol{u},\boldsymbol{v}) \to \sigma_{\mathrm{el}}(\boldsymbol{u}) : \varepsilon(\boldsymbol{v}), \quad (T,\boldsymbol{v}) \to \sigma_{\mathrm{th}}(T) : \varepsilon(\boldsymbol{v}),$$

respectively. The operator $\langle \sigma_d : \sigma_d\rangle$ *was introduced in Corollary 2.3. Finally,* $\mathcal{H}$ *denotes the mean curvature of* $\Gamma_{\mathcal{F}}$*.*

Proof. By linearity, the shape derivative of the functional $J_{\gamma,\delta}(D) = \mathbb{E}[\mathrm{VM}_{\gamma,\delta}(D)]$ into the direction of the perturbation field $\boldsymbol{\theta}$ is given as $J'_{\gamma,\delta}(D)\langle\boldsymbol{\theta}\rangle = \mathbb{E}[\mathrm{VM}'_{\gamma,\delta}](D)\langle\boldsymbol{\theta}\rangle$. Thus, in order to derive the expression of the shape derivative $J'_{\gamma,\delta}(D)\langle\boldsymbol{\theta}\rangle$, it is enough to compute the shape derivative $\mathrm{VM}'_{\gamma,\delta}(D,\omega)\langle\boldsymbol{\theta}\rangle$ and to employ Proposition 2.2 to compute its expectation.

We present the computation of $J'_{\gamma,\delta}(D)\langle\boldsymbol{\theta}\rangle$ in three steps. In order to shorten our proof, we start with the derivative $\mathrm{VM}'(D,t,\omega)\langle\boldsymbol{\theta}\rangle$, then move to the derivative

$\mathrm{VM}'_{\gamma,\delta}(D,\omega)\langle\boldsymbol{\theta}\rangle$, and finish with expression of the derivative $J'_{\gamma,\delta}(D)\langle\boldsymbol{\theta}\rangle$. In particular, to simplify the notation, we omit mentioning the random event ω in the discussion of $\mathrm{VM}'(D,t,\omega)\langle\boldsymbol{\theta}\rangle$ and $\mathrm{VM}'_{\gamma,\delta}(D,\omega)\langle\boldsymbol{\theta}\rangle$, so we assume that it is arbitrary but fixed:

$$\mathrm{VM}(D,t) \equiv \mathrm{VM}(D,t,\omega), \quad \mathrm{VM}'(D,t)\langle\boldsymbol{\theta}\rangle \equiv \mathrm{VM}'(D,t,\omega)\langle\boldsymbol{\theta}\rangle,$$

$$\mathrm{VM}_{\gamma,\delta}(D) \equiv \mathrm{VM}_{\gamma,\delta}(D,\omega), \quad \mathrm{VM}'_{\gamma,\delta}(D)\langle\boldsymbol{\theta}\rangle \equiv \mathrm{VM}'_{\gamma,\delta}(D,\omega)\langle\boldsymbol{\theta}\rangle.$$

Step 1. For sufficiently small $\boldsymbol{\theta} \in W^{1,\infty}(D_{\mathrm{box}})^d$, a change of variables in the shape functional $\mathrm{VM}(D_{\boldsymbol{\theta}},t)$ yields

$$\begin{aligned}\mathrm{VM}(D_{\boldsymbol{\theta}},t) &= \int_{D_{\boldsymbol{\theta}}} \sigma_d(\boldsymbol{u}_{D_{\boldsymbol{\theta}}}) : \sigma_d(\boldsymbol{u}_{D_{\boldsymbol{\theta}}})\,\mathrm{d}\boldsymbol{x} = 4\mu^2 \int_{D_{\boldsymbol{\theta}}} \left(\varepsilon(\boldsymbol{u}_{D_{\boldsymbol{\theta}}}) : \varepsilon(\boldsymbol{u}_{D_{\boldsymbol{\theta}}}) - 4\frac{\mathrm{div}(\boldsymbol{u}_{D_{\boldsymbol{\theta}}})^2}{d}\right)\mathrm{d}\boldsymbol{x} \\ &= 4\mu^2 \int_D \left(\boldsymbol{E}(\boldsymbol{u}_D,\boldsymbol{\theta}) : \boldsymbol{E}(\boldsymbol{u}_D,\boldsymbol{\theta}) - 4\frac{\mathrm{tr}((\boldsymbol{I}+\boldsymbol{\nabla\theta})^{-1}\nabla\boldsymbol{u}_D)^2}{d}\right)\det(\boldsymbol{I}+\nabla\boldsymbol{\theta})\,\mathrm{d}\boldsymbol{x},\end{aligned}$$

where

$$\boldsymbol{E}(\boldsymbol{v},\boldsymbol{\theta}) = \frac{1}{2}\Big((\boldsymbol{I}+\boldsymbol{\nabla\theta})^{-1}\boldsymbol{\nabla v} + \boldsymbol{\nabla v}^{\top}(\boldsymbol{I}+\boldsymbol{\nabla\theta})^{-\top}\Big).$$

By taking the derivative using Definitions 3.1 and 3.4 in the above formula, we obtain

$$\begin{aligned}\mathrm{VM}'(D,t)\langle\boldsymbol{\theta}\rangle = 4\mu^2 \int_D \Big(&2\varepsilon(\dot{\boldsymbol{u}}_D(\boldsymbol{\theta})) : \varepsilon(\boldsymbol{u}_D) - (\boldsymbol{\nabla\theta\nabla u}_D + (\boldsymbol{\nabla\theta\nabla u}_D)^{\top}) : \varepsilon(\boldsymbol{u}_D) \\ &- \frac{8}{d}\,\mathrm{div}(\boldsymbol{u}_D)(\mathrm{div}(\dot{\boldsymbol{u}}_D) - \mathrm{tr}(\boldsymbol{\nabla\theta\nabla u}_D)) \\ &+ \mathrm{div}(\boldsymbol{\theta})\left(\varepsilon(\boldsymbol{u}_{D_{\boldsymbol{\theta}}}) : \varepsilon(\boldsymbol{u}_D) - 4\frac{\mathrm{div}(\boldsymbol{u}_D)^2}{d}\right)\Big)\,\mathrm{d}\boldsymbol{x} \\ = \int_D \Big(&2\sigma_d(\dot{\boldsymbol{u}}_D(\boldsymbol{\theta})) : \sigma_d(\boldsymbol{u}_D) - 4\mu\sigma_d(\boldsymbol{u}_D) : (\nabla\boldsymbol{\theta}\nabla\boldsymbol{u}) \\ &+ \mathrm{div}(\boldsymbol{\theta})\sigma_d(\boldsymbol{u}_D) : \sigma_d(\boldsymbol{u}_D)\Big)\,\mathrm{d}\boldsymbol{x}.\end{aligned} \tag{3.14}$$

In order to simplify the expression for $\mathrm{VM}'(D,t)\langle\boldsymbol{\theta}\rangle$, we introduce adjoint states. First, in order to characterize $\dot{\boldsymbol{u}}$ in (3.14), we formulate the variational identity for the adjoint state $\boldsymbol{w}_D \in H((0,t_f),D)$ as follows

$$\int_0^{t_f}\int_D \sigma_{\mathrm{el}}(\boldsymbol{w}_D) : \varepsilon(\boldsymbol{v})\,\mathrm{d}\boldsymbol{x}\,\mathrm{d}t = 4\mu\int_0^{t_f}\int_D \sigma_d(\boldsymbol{u}_D) : \varepsilon(\boldsymbol{v})\,\mathrm{d}\boldsymbol{x}\,\mathrm{d}t \quad \text{for any} \quad \boldsymbol{v} \in H((0,t_f),D). \tag{3.15}$$

By taking $\dot{\boldsymbol{u}}$ as test function in (3.15) and $\boldsymbol{w}_D$ as test function in (3.9), we conclude

$$2\int_0^{t_f}\int_D \sigma_d(\dot{\boldsymbol{u}}_D(\boldsymbol{\theta})) : \sigma_d(\boldsymbol{u}_D)\,\mathrm{d}\boldsymbol{x}\,\mathrm{d}t$$

$$= 4\mu \int_0^{t_f} \int_D \sigma_d(\boldsymbol{u}_D) : \varepsilon(\dot{\boldsymbol{u}}_D(\boldsymbol{\theta}))\,\mathrm{d}\boldsymbol{x}\,\mathrm{d}t = \int_0^{t_f} \int_D \sigma_{\mathrm{el}}(\dot{\boldsymbol{u}}_D(\boldsymbol{\theta})) : \varepsilon(\boldsymbol{w}_D)\,\mathrm{d}\boldsymbol{x}\,\mathrm{d}t$$

$$\begin{aligned} = \int_0^{t_f} \int_D \Big(& \mathbb{C} : (\boldsymbol{\nabla\theta\nabla u}_D) : \boldsymbol{\nabla w}_D + \mathbb{C} : \boldsymbol{\nabla u}_D : (\boldsymbol{\nabla\theta\nabla w}_D) - \mathrm{div}(\boldsymbol{\theta})\sigma_{\mathrm{el}}(\boldsymbol{u}_D) : \varepsilon(\boldsymbol{w}_D) \\ & + \mathrm{div}(\boldsymbol{f} \otimes \boldsymbol{\theta}) \cdot \boldsymbol{w}_D - \dot{T}_D(\boldsymbol{\theta})\boldsymbol{B} : \boldsymbol{\nabla w}_D + (T_D - T_{\mathrm{in}})\boldsymbol{B}\boldsymbol{\nabla\theta}^\top : \boldsymbol{\nabla w}_D \\ & - \mathrm{div}(\boldsymbol{\theta})\sigma_{\mathrm{th}}(T_D) : \varepsilon(\boldsymbol{w}_D) \Big)\,\mathrm{d}\boldsymbol{x}\,\mathrm{d}t. \end{aligned}$$

With this identity at hand, we can transform (3.14) into

$$\begin{aligned} \mathrm{VM}'(D,t)\langle\boldsymbol{\theta}\rangle = \int_D \Big(& \mathbb{C} : (\boldsymbol{\nabla\theta\nabla u}_D) : \boldsymbol{\nabla w}_D + \mathbb{C} : \boldsymbol{\nabla u}_D : (\boldsymbol{\nabla w}_D\boldsymbol{\nabla\theta}) \\ & - \mathrm{div}(\boldsymbol{\theta})\sigma_{\mathrm{el}}(\boldsymbol{u}_D) : \varepsilon(\boldsymbol{w}_D) + \mathrm{div}(\boldsymbol{f} \otimes \boldsymbol{\theta}) \cdot \boldsymbol{w}_D \\ & - \dot{T}_D(\boldsymbol{\theta})\boldsymbol{B} : \boldsymbol{\nabla w}_D + (T_D - T_{\mathrm{in}})\boldsymbol{B}\boldsymbol{\nabla\theta}^\top : \boldsymbol{\nabla w}_D \\ & - \mathrm{div}(\boldsymbol{\theta})\sigma_{\mathrm{th}}(T_D) : \varepsilon(\boldsymbol{w}_D) - 4\mu\sigma_d(\boldsymbol{u}_D) : (\nabla\boldsymbol{\theta}\nabla\boldsymbol{u}) \\ & + \mathrm{div}(\boldsymbol{\theta})\sigma_d(\boldsymbol{u}_D) : \sigma_d(\boldsymbol{u}_D) \Big)\,\mathrm{d}\boldsymbol{x}. \end{aligned} \tag{3.16}$$

Step 2. In this step, we move to the computation of the derivative $\mathrm{VM}'_{\gamma,\delta}(D)\langle\boldsymbol{\theta}\rangle$. Note that

$$\mathrm{VM}'_{\gamma,\delta}(D)\langle\boldsymbol{\theta}\rangle = \gamma \int_0^{t_f} \mathrm{VM}'(D,t)\langle\boldsymbol{\theta}\rangle\,\mathrm{d}t + \delta\,\mathrm{VM}'(D,t_f)\langle\boldsymbol{\theta}\rangle. \tag{3.17}$$

In order to eliminate $\dot{T}$, we introduce a variational identity for the adjoint state $p_D \in P_\delta((0,t_f),D)$ in accordance with

$$\begin{aligned} & \int_0^{t_f} \int_D \rho\frac{\partial p_D}{\partial t} r\,\mathrm{d}\boldsymbol{x}\,\mathrm{d}t - \int_0^{t_f} \int_D k\nabla p_D \cdot \nabla r\,\mathrm{d}\boldsymbol{x}\,\mathrm{d}t - \int_0^{t_f} \int_{\Gamma_{\mathcal{F}}} \beta p_D r\,\mathrm{d}\boldsymbol{s}\,\mathrm{d}t \\ & \quad = -\gamma \int_0^{t_f} \int_D r\boldsymbol{B} : \boldsymbol{\nabla w}_D\,\mathrm{d}\boldsymbol{x}\,\mathrm{d}t \quad \text{for any} \quad r \in L^2((0,t_f); H^1_{\mathcal{D}}(D)). \end{aligned} \tag{3.18}$$

Remark that, in case of the heat equation, the adjoint state equation is inverse in time. Thus, we assume that

$$p_{f,D} := p_D(t_f) = \delta\boldsymbol{B} : \boldsymbol{\nabla w}_{f,D}.$$

It is easy to check that the variational formulations (3.15) and (3.18) correspond to the boundary value problems (3.12) and (3.13), respectively. By taking $\dot{T}$ as a test function after integration by parts in the first term of (3.18), and p_D as test function in (3.5), we arrive at

$$\gamma \int_0^{t_f} \int_D \dot{T}_D(\boldsymbol{\theta})\boldsymbol{B} : \boldsymbol{\nabla w}_D\,\mathrm{d}\boldsymbol{x}\,\mathrm{d}t + \delta \int_D \dot{T}_{f,D}(\boldsymbol{\theta})\boldsymbol{B} : \boldsymbol{\nabla w}_{f,D}\,\mathrm{d}\boldsymbol{x}$$

$$
\begin{aligned}
&= \int_0^{t_f}\int_D \rho\frac{\partial \dot{T}_D(\boldsymbol{\theta})}{\partial t} p_D \,\mathrm{d}\boldsymbol{x}\,\mathrm{d}t + \int_0^{t_f}\int_D k\nabla p_D\cdot\nabla\dot{T}_D(\boldsymbol{\theta})\,\mathrm{d}\boldsymbol{x}\,\mathrm{d}t - \int_0^{t_f}\int_{\Gamma_{\mathcal{F}}} \beta p_D\dot{T}_D(\boldsymbol{\theta})\,\mathrm{d}\boldsymbol{s}\,\mathrm{d}t\\
&= \int_0^{t_f}\int_D \mathrm{div}(Q\boldsymbol{\theta})p_D\,\mathrm{d}\boldsymbol{x}\,\mathrm{d}t + \int_0^{t_f}\int_{\Gamma_{\mathcal{F}}}\mathrm{div}_{\boldsymbol{\tau}}(\beta\widetilde{T}\boldsymbol{\theta})p_D\,\mathrm{d}\boldsymbol{s}\,\mathrm{d}t - \int_0^{t_f}\int_D \mathrm{div}(\boldsymbol{\theta})\rho\frac{\partial T_D}{\partial t}p_D\,\mathrm{d}\boldsymbol{x}\,\mathrm{d}t\\
&\quad - \int_0^{t_f}\int_D k\boldsymbol{A}'(\boldsymbol{\theta})\nabla T_D\cdot\nabla p_D\,\mathrm{d}\boldsymbol{x}\,\mathrm{d}t - \int_0^{t_f}\int_{\Gamma_{\mathcal{F}}}\mathrm{div}_{\boldsymbol{\tau}}(\boldsymbol{\theta})\,\beta T_D p_D\,\mathrm{d}\boldsymbol{s}\,\mathrm{d}t.
\end{aligned}
$$

Thus, by using the identity above from (3.16) and (3.17), we derive the expression

$$
\begin{aligned}
\mathrm{VM}'_{\gamma,\delta}(D)\langle\boldsymbol{\theta}\rangle &= \gamma\int_0^{t_f}\mathrm{VM}'_1(D,t)\langle\boldsymbol{\theta}\rangle\,\mathrm{d}t + \delta\,\mathrm{VM}'_1(D,t_f)\langle\boldsymbol{\theta}\rangle\\
&\quad + \int_0^{t_f}\int_D\Big(\mathrm{div}(Q\boldsymbol{\theta})p_D - \mathrm{div}(\boldsymbol{\theta})\rho\frac{\partial T_D}{\partial t}p_D - k\boldsymbol{A}'(\boldsymbol{\theta})\nabla T_D\cdot\nabla p_D\Big)\,\mathrm{d}\boldsymbol{x}\,\mathrm{d}t\\
&\quad + \int_0^{t_f}\int_{\Gamma_{\mathcal{F}}}\Big[\mathrm{div}_{\boldsymbol{\tau}}(\beta\widetilde{T}\boldsymbol{\theta})p_D - \mathrm{div}_{\boldsymbol{\tau}}(\boldsymbol{\theta})\beta T_D p_D\Big]\,\mathrm{d}\boldsymbol{s}\,\mathrm{d}t,
\end{aligned}
\tag{3.19}
$$

where

$$
\begin{aligned}
\mathrm{VM}'_1(D,t)\langle\boldsymbol{\theta}\rangle := \int_D\Big(&\mathbb{C}:(\boldsymbol{\nabla\theta}\boldsymbol{\nabla}\boldsymbol{u}_D):\boldsymbol{\nabla}\boldsymbol{w}_D + \mathbb{C}:\boldsymbol{\nabla}\boldsymbol{u}_D:(\boldsymbol{\nabla\theta}\boldsymbol{\nabla}\boldsymbol{w}_D)\\
&- \mathrm{div}(\boldsymbol{\theta})\sigma_{\mathrm{el}}(\boldsymbol{u}_D):\varepsilon(\boldsymbol{w}_D) + \mathrm{div}(\boldsymbol{f}\otimes\boldsymbol{\theta})\cdot\boldsymbol{w}_D\\
&+ (T_D - T_{\mathrm{in}})\boldsymbol{B}\boldsymbol{\nabla\theta}^{\top}:\boldsymbol{\nabla}\boldsymbol{w}_D - \mathrm{div}(\boldsymbol{\theta})\sigma_{\mathrm{th}}(T_D):\varepsilon(\boldsymbol{w}_D)\\
&- 4\mu\sigma_d(\boldsymbol{u}_D):(\nabla\boldsymbol{\theta}\nabla\boldsymbol{u}) + \mathrm{div}(\boldsymbol{\theta})\sigma_d(\boldsymbol{u}_D):\sigma_d(\boldsymbol{u}_D)\Big)\,\mathrm{d}\boldsymbol{x}.
\end{aligned}
$$

Under the hypotheses stated above and thanks to Theorem 3.5, we can consider that $\boldsymbol{\theta} = (\theta\cdot\boldsymbol{n})\boldsymbol{n}$ on $\Gamma_{\mathcal{F}}$. Hence, we conclude that $\mathrm{div}_{\boldsymbol{\tau}}(\boldsymbol{\theta}) = \mathcal{H}(\boldsymbol{\theta}\cdot\boldsymbol{n})$. Therefore, by applying Green's formula and the identitiy (3.19), we achieve the boundary integral form of $\mathrm{VM}_{\gamma,\delta}(D)$:

$$
\begin{aligned}
\mathrm{VM}_{\gamma,\delta}(D)\langle\boldsymbol{\theta}\rangle &= \gamma\int_0^{t_f}\mathrm{VM}'_2(D,t)\langle\boldsymbol{\theta}\rangle\,\mathrm{d}t + \delta\,\mathrm{VM}'_2(D,t_f)\langle\boldsymbol{\theta}\rangle\\
&\quad + \int_0^{t_f}\int_{\Gamma_{\mathcal{F}}}\Big(k\frac{\partial T_D}{\partial\boldsymbol{n}}\frac{\partial p_D}{\partial\boldsymbol{n}} - k\nabla T_D\cdot\nabla p_D - \rho\frac{\partial T_D}{\partial t}p_D\\
&\qquad - \beta\frac{\partial\widetilde{T}}{\partial\boldsymbol{n}}p_D + Qp_D + \mathcal{H}\beta(\widetilde{T}-T_D)p_D\Big)(\boldsymbol{\theta}\cdot\boldsymbol{n})\,\mathrm{d}\boldsymbol{s}\,\mathrm{d}t,
\end{aligned}
\tag{3.20}
$$

where

$$
\mathrm{VM}'_2(D,t)\langle\boldsymbol{\theta}\rangle := \int_{\Gamma_{\mathcal{F}}}\Big(\sigma_{\mathrm{el}}(\boldsymbol{w}_D)\boldsymbol{n}\cdot\frac{\partial\boldsymbol{u}_D}{\partial\boldsymbol{n}} + \sigma_{\mathrm{el}}(\boldsymbol{u}_D)\boldsymbol{n}\cdot\frac{\partial\boldsymbol{w}_D}{\partial\boldsymbol{n}} - \sigma_{\mathrm{el}}(\boldsymbol{u}_D):\varepsilon(\boldsymbol{w}_D)
$$

$$+ \boldsymbol{f} \cdot \boldsymbol{w}_D + \sigma_{\mathrm{th}}(T_D)\boldsymbol{n} \cdot \frac{\partial \boldsymbol{w}_D}{\partial \boldsymbol{n}} - \sigma_{\mathrm{th}}(T_D) : \varepsilon(\boldsymbol{w}_D)$$
$$- 4\mu\sigma_d(\boldsymbol{u}_D)\boldsymbol{n} \cdot \frac{\partial \boldsymbol{u}_D}{\partial \boldsymbol{n}} + \sigma_d(\boldsymbol{u}_D) : \sigma_d(\boldsymbol{u}_D)\Big)(\boldsymbol{\theta} \cdot \boldsymbol{n})\,\mathrm{d}\boldsymbol{s}.$$

By using the boundary conditions in (2.1), (2.2), (3.12), and (3.13), we immediately obtain the final expression of $\mathrm{VM}_{\gamma,\delta}(D)$ from (3.20)

$$\begin{aligned}
&\mathrm{VM}_{\gamma,\delta}(D)\langle\boldsymbol{\theta}\rangle \\
&= \gamma \int_0^{t_f} \int_{\Gamma_{\mathcal{F}}} \Big(\boldsymbol{f} \cdot \boldsymbol{w}_D - \sigma(\boldsymbol{u}_D, T_D) : \varepsilon(\boldsymbol{w}_D) + \sigma_d(\boldsymbol{u}_D) : \sigma_d(\boldsymbol{u}_D)\Big)(\boldsymbol{\theta} \cdot \boldsymbol{n})\,\mathrm{d}\boldsymbol{x}\,\mathrm{d}t \\
&+ \delta \int_{\Gamma_{\mathcal{F}}} \Big(\boldsymbol{f}_f \cdot \boldsymbol{w}_{f,D} - \sigma(\boldsymbol{u}_{f,D}, T_{f,D}) : \varepsilon(\boldsymbol{w}_{f,D}) + \sigma_d(\boldsymbol{u}_{f,D}) : \sigma_d(\boldsymbol{u}_{f,D})\Big)(\boldsymbol{\theta} \cdot \boldsymbol{n})\,\mathrm{d}\boldsymbol{x}\,\mathrm{d}t \\
&+ \int_0^{t_f} \int_{\Gamma_{\mathcal{F}}} \Big(\beta\Big(\mathcal{H} - \frac{2\beta}{k}\Big)(\widetilde{T} - T_D)p_D - \beta\frac{\partial \widetilde{T}}{\partial \boldsymbol{n}}p_D + Qp_D - \rho\frac{\partial T_D}{\partial t}p_D \\
&\qquad\qquad - k\nabla T_D \cdot \nabla p_D\Big)(\boldsymbol{\theta} \cdot \boldsymbol{n})\,\mathrm{d}\boldsymbol{x}\,\mathrm{d}t.
\end{aligned} \tag{3.21}$$

Step 3. To complete the proof, we recall that the field $\boldsymbol{u}_D$ of displacement and the temperature T_D are random. Consequently, the adjoint states $\boldsymbol{w}_D$ and p_D are also random. Nonetheless, the derivative $\mathrm{VM}_{\gamma,\delta}(D,\omega)\langle\boldsymbol{\theta}\rangle$ is a bilinear form. Thus, by applying Proposition 2.2 to (3.21), it is easy to derive the statement (3.11) and to conclude the proof. □

The resulting expression opens up the possibility of using gradient-based algorithms that have proven to be effective for the numerical solution of shape optimization problems.

4 Numerical realization

In this part, we discuss the numerical methods and algorithms for solving the problem under consideration. We use the level-set method to numerically solve the shape optimization problem. The random temperature is modeled by means of the Karhunen–Loéve expansion. We present numerical experiments for the optimization of a bridge-type structure under the action of a random heat wave.

4.1 Level-set method

A major challenge in the implementation shape optimization algorithms is the accurate representation of shapes. To address this, we use the level-set method, originally introduced in [23] and adapted for shape optimization in [5].

In this method, the domain $D \subset D_{\text{box}}$ is given by the subset of negative function values of a *level-set function* $\phi : D_{\text{box}} \to \mathbb{R}$, which means that

$$\begin{cases} \phi(\boldsymbol{x}) < 0 & \text{if } \boldsymbol{x} \in D, \\ \phi(\boldsymbol{x}) = 0 & \text{if } \boldsymbol{x} \in \partial D, \\ \phi(\boldsymbol{x}) > 0 & \text{if } \boldsymbol{x} \in D_{\text{box}} \setminus \overline{D}. \end{cases}$$

The discretized motion of the domain D in D_{box} translates in accordance with

$$\begin{cases} \phi_{n+1} = \phi_n - t_n \boldsymbol{\theta}_n \cdot \nabla \phi_n & \text{in } D_{\text{box}}, \\ \phi_0 = \phi_{\text{in}} & \text{in } D_{\text{box}}, \end{cases}$$

where $t_n = \text{const} > 0$ is the discretization step size, ϕ_{in} is a chosen initial level-set function, and $\boldsymbol{\theta}_n$ is the velocity field.

This velocity field is determined by a constrained optimization algorithm using knowledge of the shape gradient of the objective and the constraint. The natural idea is to use the projected gradient. Here, we use instead an alternative: the null-space algorithm introduced by Feppon et al. in [16] which has become popular in numerical shape optimization. This algorithm starts from a point that does not satisfy the constraint, and seeks to orientate the direction of the deformation at each step in such a way that the constrained is fulfilled first, while the objective is reduced if possible. Interested readers are referred to the article [16] for a precise definition of the algorithm and a study of its properties.

This algorithm requires the computation of the shape gradient of both the objective functional and the constraint. This is achieved by the usual extension-regularization procedure, discussed by de Gournay in [14] for example, motivating the use of the formulas for shape derivatives introduced in Theorem 3.8 and Proposition 3.10. We use the Dapogny-Feppon implementation of the null-space optimization algorithm, see [13]. The boundary values problem are solved with the finite element solver FreeFem++, see [18].

4.2 Computation of second-order moments

Calculating the derivative $J'_{\gamma,\delta}(D)\langle\boldsymbol{\theta}\rangle$ becomes much more complicated in comparison to calculating the derivative $\text{Vol}'(D)\langle\boldsymbol{\theta}\rangle$, since it involves the computation of first and second order moments of the states and their adjoints. Thanks to the linearity of the governing equation and its adjoint, it is straightforward to calculate values like $\mathbb{E}[\boldsymbol{w}]$ and $\mathbb{E}[p]$ if the expectation of the data $\widetilde{T}$ is known. In contrast, the computation of $\text{Cor}[\boldsymbol{u}, \boldsymbol{u}]$, $\text{Cor}[\boldsymbol{u}, \boldsymbol{w}]$, etc. is more involved.

One way to compute such expresssions is to rely on the low-rank approximation of the two-point correlation functions. To do so, we should assume that $\text{Cor}[\widetilde{T}, \widetilde{T}]$ is given. Then, we can approximate $\widetilde{T}(t, \boldsymbol{x}, \omega)$ by the truncated Karhunen–Loéve expansion

$$\widetilde{T}(t, \boldsymbol{x}, \omega) \approx \sum_{k=1}^{M} \xi_k(\omega) \otimes \widetilde{T}_k(t, \boldsymbol{x}), \tag{4.1}$$

where the random variables $\{\xi_k\}$ are orthonormal with respect to $L^2_{\mathbb{P}}(\Omega)$ and the spatial functions $\{\widetilde{T}_k\}$ are orthonormal with respect to $L^2(D)$, see [17, 20] for example. Thus, by linearity, there holds

$$T_D(t, \boldsymbol{x}, \omega) \approx \sum_{k=1}^{M} \xi_k(\omega) \otimes T_{D,k}(t, \boldsymbol{x}),$$

where $T_{D,k}$ corresponds to the solution of the heat equation for the input $\widetilde{T}_k(t, \boldsymbol{x})$. Analogue expansions hold true for the displacement field $\boldsymbol{u}_D$ and the adjoint states p_D and $\boldsymbol{w}_D$. By inserting the respective extension and exploiting the orthonormality of the random variables, it is easily seen that the correlation of $\boldsymbol{u}_D$ is approximated through

$$\mathrm{Cor}[\boldsymbol{u}_D, \boldsymbol{u}_D]((t, \boldsymbol{x}), (t', \boldsymbol{x}')) \approx \sum_{k=1}^{M} \boldsymbol{u}_{D,k}(t, \boldsymbol{x}) \otimes \boldsymbol{u}_{D,k}(t', \boldsymbol{x}').$$

This can be used to compute the expression of the form

$$\langle \sigma_d : \sigma_d \rangle \mathrm{Cor}[\boldsymbol{u}_D, \boldsymbol{u}_D]((t, \boldsymbol{x}), (t', \boldsymbol{x}')) \approx \sum_{k=1}^{M} \sigma_d(\boldsymbol{u}_{D,k}(t, \boldsymbol{x})) : \sigma_d(\boldsymbol{u}_{D,k}(t', \boldsymbol{x}')).$$

Similar expressions can be derived for $\langle \sigma_{\mathrm{el}} : \varepsilon \rangle \mathrm{Cor}[\boldsymbol{u}_D, \boldsymbol{w}_D]$ and $\langle \sigma_{\mathrm{th}} : \varepsilon \rangle \mathrm{Cor}[T_D, \boldsymbol{w}_D]$ that are also present in the expression for the shape derivative $J'_{\gamma,\delta}(D)\langle \boldsymbol{\theta} \rangle$, see (3.11).

In the end, we reduced the problem of computing the shape derivative $J'_{\gamma,\delta}(D)\langle \boldsymbol{\theta} \rangle$by means of second-order moments to the problem of determining $\widetilde{T}_k,\ k = 1, \ldots, M$ in (4.1). In order to determine these, we compute a truncated spectral decomposition

$$\mathrm{Cor}[\widetilde{T}, \widetilde{T}]((t, \boldsymbol{x}), (t', \boldsymbol{x}')) \approx \sum_{k=1}^{M} \lambda_k \phi_k(t, \boldsymbol{x}) \otimes \phi_k(t', \boldsymbol{x}'),$$

where $(\lambda_k, \phi_k),\ k = 1 \ldots, M$ are the eigenpairs of the associated Hilbert–Schmidt operator

$$\phi \mapsto \int_0^{t_f} \int_D \mathrm{Cor}[\widetilde{T}, \widetilde{T}]((\cdot, \cdot), (t', \boldsymbol{x}'))\phi(t', \boldsymbol{x}') \, \mathrm{d}\boldsymbol{x}' \, \mathrm{d}t'.$$

Thus, there holds $\widetilde{T}_k(t, \boldsymbol{x}) = \sqrt{\lambda_k}\phi_k(t, \boldsymbol{x}),\ k = 1, \ldots, M$. The efficient numerical realization is presented in [17].

4.3 Computational model

The external domain $D_{\mathrm{box}} \in \mathbb{R}^2$ is chosen as the square 1cm × 1cm. Since the mesh is automatically adapted towards the current geometry during the optimization process, it is sufficient to say that the finite element size changes from $h_{\min} = 0.01$ to $h_{\max} = 0.02$. The initial mesh is presented in Figure 4.1.

The final time is taken as $t_f = 1$. We solve the dynamic problems (2.1) and (3.13) by using the Crank–Nicolson scheme. In order to deal with the incompatible boundary

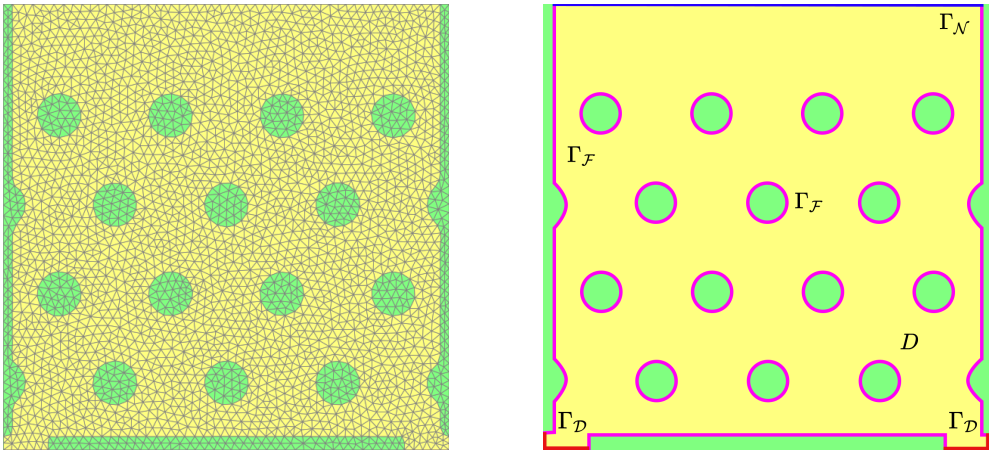

(a) (b)

Figure 4.1: Initial setting. (a) Triangulation and (b) boundary conditions.

conditions in the ajoint equation (3.13), we apply a grading in the time discretization. To this end, we split the time interval $(0, t_f)$ into 20 subintervals, where the first 15 subintervals are of the fixed with h_t, while the size of the last 5 subintervals is decreasing towards the end with the factor $1/2$, i.e., our time steps looks like $h_t/2, h_t/4, \ldots, h_t/32$.

The parameters in the thermoelasticity model are chosen as follows: Young's modulus $E = 200$ GPa, Poisson's ratio $\nu = 0.3$, material density $\tilde{\rho} = 8000\,\mathrm{kg\,m^{-2}}$, specific heat capacity $\tilde{C} = 450\,\mathrm{J\,kg^{-1}}$, thermal expansion coefficient $\alpha = 15 \cdot 10^{-6}\,\mathrm{°C^{-1}}$, thermal conductivity coefficient $k = 15\,\mathrm{W\,m^{-2}\,°C^{-1}}$, and heat transfert coefficient $\beta = 10\,\mathrm{W\,m^{-2}\,°C^{-1}}$. The body force is $\boldsymbol{f} = (0, 0)$ and the surface force is $\boldsymbol{g} = (0, -0.25)$. The initial temperature is taken as $T_{\mathrm{in}} = 0\,\mathrm{°C}$.

The external temperature is taken as a heat wave that traveles bottom-up through D_{box}, which is subject to random perturbations. The uncertainties are defined through the following correlation function, which is the product of a Matérn kernel (see [22]) in space and a Gaussian kernel in time

$$\mathrm{Cor}[\widetilde{T}, \widetilde{T}]((t, \boldsymbol{x}), (t', \boldsymbol{x}')) := K_{\mathrm{Gauss}}(|t - t'|) K_{\mathrm{Mat},5/2}(\|\boldsymbol{x} - \boldsymbol{x}'\|), \tag{4.2}$$

where

$$K_{\mathrm{Mat},5/2}(r) := \big(1 + \sqrt{5}r + 5r^2\big) \exp\big(-\sqrt{5}r\big) \quad \text{and} \quad K_{\mathrm{Gauss}}(r) := \frac{\exp(-r^2/2)}{\sqrt{2\pi}}.$$

Then, the temperature $\widetilde{T}$ is given by

$$\widetilde{T}(t, \boldsymbol{x}, \omega) := \widetilde{T}_{\mathrm{det}}(t, \boldsymbol{x}) + \kappa \widetilde{T}_{\mathrm{stoch}}(t, \boldsymbol{x}, \omega),$$

where $\widetilde{T}_{\mathrm{det}}(t, \boldsymbol{x}) := \max\{0, -600 \sin(x_2 - 2\pi t)\}$ and

$$\widetilde{T}_{\mathrm{stoch}}(t, \boldsymbol{x}, \omega) := \sum_{i=1}^{48} \sqrt{\lambda_i} \phi_i(t, \boldsymbol{x}) \xi_i(\omega).$$

is obtained by computing (4.1) up to a relative error of the size 10^{-3}. The parameter $\kappa > 0$ allows us to control the size of the random fluctuations and is chosen such that

$$\frac{\|\widetilde{T}_{\text{stoch}}\|_{L^2((0,t_f),D_{\text{box}})}}{\|\widetilde{T}_{\text{det}}\|_{L^2((0,t_f),D_{\text{box}})}} \approx 0.3.$$

i.e., there is about 30% random noise in the data. A visualization of $\widetilde{T}_{\text{det}}(t,\boldsymbol{x})$ and $\widetilde{T}(t,\boldsymbol{x},\omega^*)$ for some random sample ω^* at different time steps can be found in Figure 4.2. Note that $\widetilde{T}$ is defined in the whole domain D_{box} but only its restriction on the boundary $\Gamma_{\mathcal{F}} \cup \Gamma_{\mathcal{N}}$ is used.

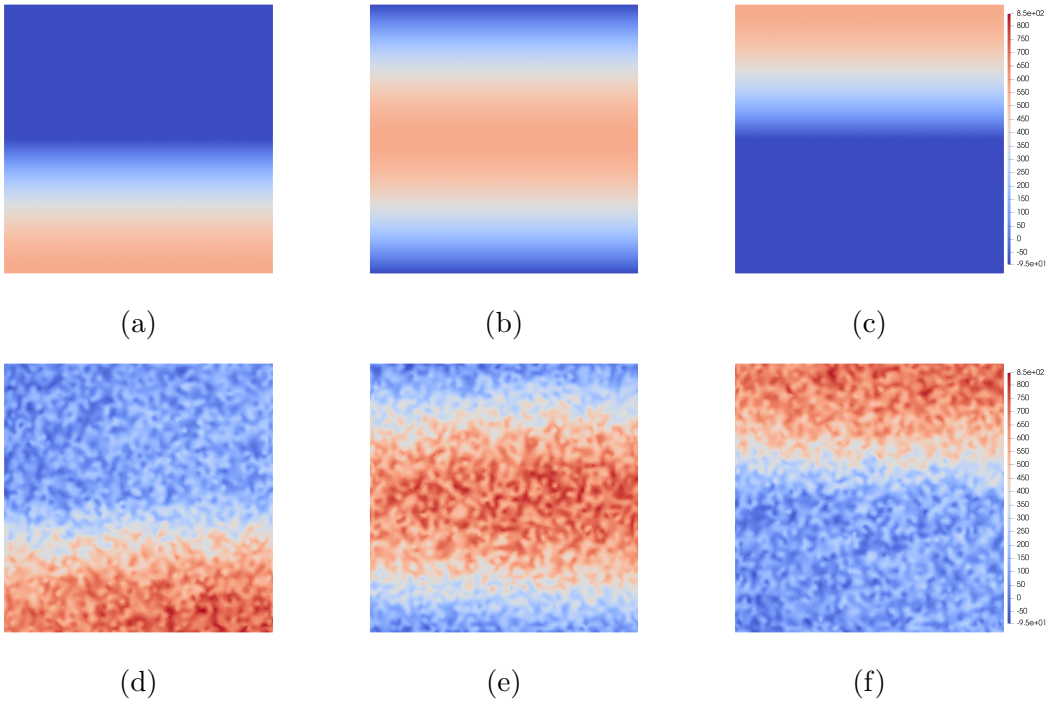

(a) (b) (c)

(d) (e) (f)

Figure 4.2: Deterministic external temperature (top row) and a specific sample of its random counterpart (bottom row) at time $t = 0.25$: (a), (d); $t = 0.5$: (b), (e); $t = 0.75$: (c), (f).

4.4 Numerical results

First, we shall study the magnitude of the effect of the uncertainty term. To this end, we have perform two experiments for the situation $\gamma = 1$ and $\delta = 0$, which means that we work only with time-averaged shape functional. In the first experiment, we consider no uncertainty, i.e., there holds $\widetilde{T} \equiv \widetilde{T}_{\text{det}}$ and we obtain the shape functional $\text{VM}_{1,0}(D)$. In the second experiment, we use $\widetilde{T}(\omega)$ which we take as described above. In this case, the shape functional becomes $J_{1,0}(D)$. The threshold for $\text{VM}_{1,0}(D)$ and

$J_{1,0}(D)$, respectively, is set to $\tau = 0.15$ and the optimization procedure is halted after 250 iterations. The results are presented in the Figure 4.3.

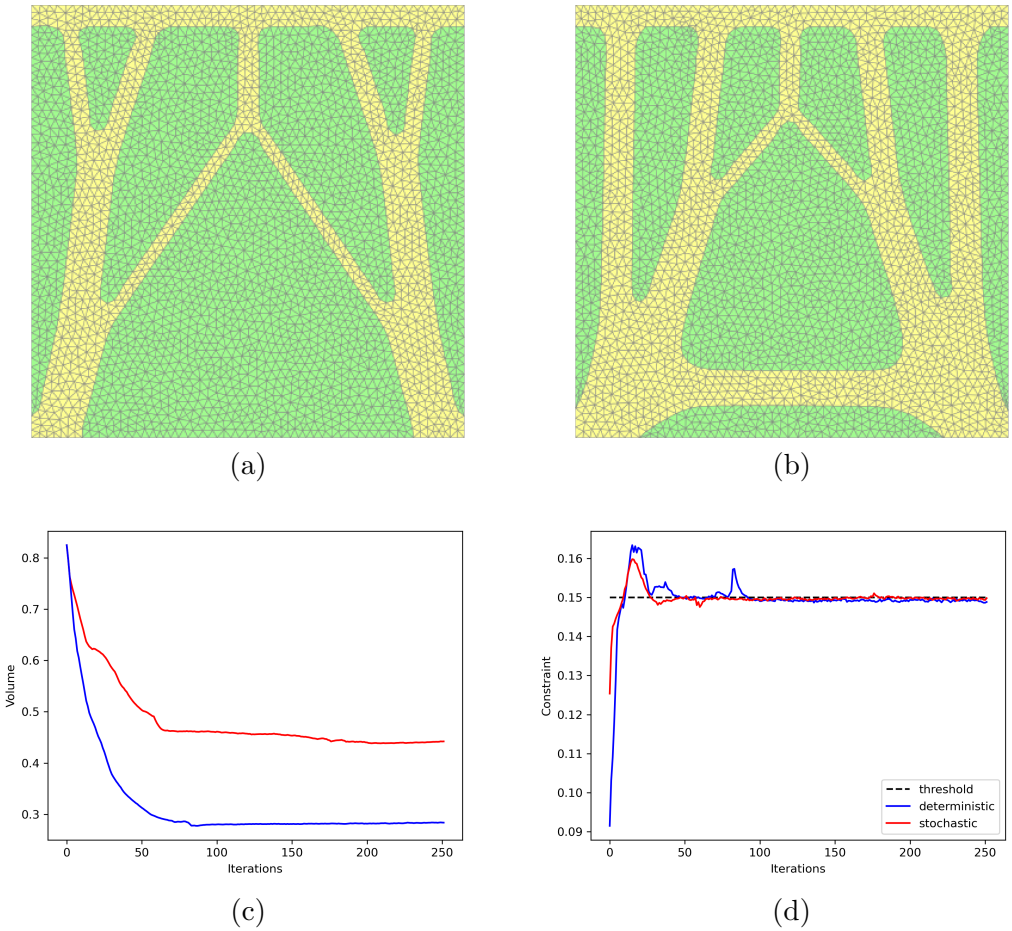

Figure 4.3: Impact of uncertainty. Top row: (a) final shape in deterministic case, (b) final shape in stochastic case. Bottom row: convergence histories (blue: deterministic, red: random) (c) objective functional Vol(D), (d) constrainted functionals $\mathrm{VM}_{1,0}(D)$ and $J_{1,0}(D)$.

As we can see, when uncertainties are taken into account, a thicker part of the design appears to make it more robust. It is rather reasonable since we are considering large uncertainties, which make the temperature distribution more chaotic. In the graphs, we observe the convergence of the optimization procedure, which validates the feasibility of the approach and the numerical method that was proposed.

Next, we consider different cases of parameter choices for γ and δ to see what effect the von Mises stress at the end of the time interval has on the optimal shape. For this purpose, we perform two more experiments with uncertainties: one for the choice $\gamma = \delta = 0.5$ and another one with the choice $\gamma = 0$ and $\delta = 1$. The former one corresponds to an equal consideration of the constraint averaged in time and evaluated

at the final instant. Conversely, in the latter one, only the value of the functional at the final time t_f is taken into account. The threshold and the number of iterations is set as before. The results are shown in Figure 4.4.

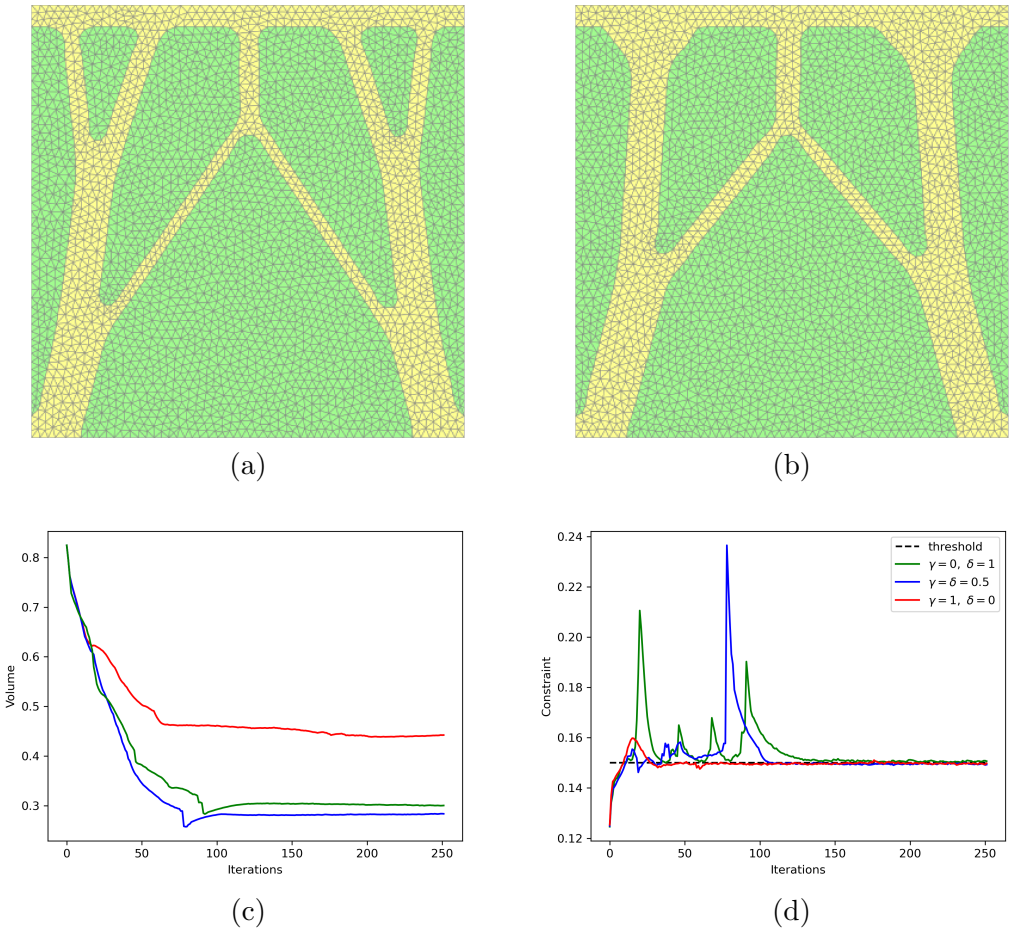

Figure 4.4: Impact of weights. Top row: (a) final shape in the case with $\gamma = \delta = 0.5$, (b) final shape in the case with $\gamma = 0,\ \delta = 1$. Bottom row: convergence histories (green: $\gamma = 0,\ \delta = 1$, blue: $\gamma = \delta = 0.5$, red: $\gamma = 1,\ \delta = 0$) (c) objective functional Vol(D), (d) constrainted functionals $J_{0,1}(D)$, $J_{0.5,0.5}(D)$ and $J_{1,0}(D)$.

As we can see in Figure 4.4, the results obey the following logic. Since the heat wave moves from the bottom to the top, the stress concentration at the final time will be accumulated in the upper part of the structure. Therefore, the upper part of the structure is reinforced as δ increases. Indeed, a comparison with Figure 4.3 (b) confirms this observation. Therein, only the time-averaged functional is considered and hence the shape functional is under a uniform influence of the von Mises stress at different moments of time. Thus, in this case, a robust reinforcement is required in the whole structure.

The convergence histories of the algorithm are shown in the graphs in Figure 4.4

(c) and (d) in cases with different weights γ and δ. The peaks observed in subplot (d) correspond to changes in topology during optimization procedure. These jumps occur since the distribution of the temperature between different areas is different, so there will be singularities if such areas merge.

5 Conclusion

The present article dealt with a shape optimization problem for a thermoelasticity model with uncertainties in the Robin boundary condition. The problem was formulated as the minimization of the body's volume under an inequality constraint on the expectation of the combination of the time-averaged L^2-norm of the von Mises stress and taken at last time. We derived an analytical expressions of the expected shape functional and its shape derivative via second-order correlations. An efficient numerical method based on low-rank approximation was proposed. The solution of the optimization problem was numerically implemented via the level-set method. The results of numerical experiments in two spatial dimensions were presented, validating the feasibility of the present approach.

The limitations of this model are contingent upon the extent of thermal variations. When such variations are significant, the coefficients that describe the properties of the materials (dilation, thermal conduction, Young's modulus, etc.) are not constant and depend on the temperature. In the present theromoelastic model, however, we have neglected this dependence. Accounting for it will be the subject of further research.

Acknowledgement

This research has been in parts performed while H.H. was visiting the Laboratory of Mathematics and its Applications of PAU – UMR CNRS 5142. The hospitality and the support are gratefully acknowledged.

References

[1] Gregoire Allaire and Charles Dapogny. A linearized approach to worst-case design in parametric and geometric shape optimization. *Mathematical Models and Methods in Applied Sciences*, 24:2199–2257, 2014.

[2] Gregoire Allaire and Charles Dapogny. A deterministic approximation method in shape optimization under random uncertainties. *SMAI Journal of computational mathematics*, 1:83–143, 2015.

[3] Grégoire Allaire, Charles Dapogny, and François Jouve. Shape and topology optimization. In *Handbook of Numerical Analysis*, volume 22, pages 1–132. Elsevier, Amsterdam, 2021.

[4] Grégoire Allaire and Lukas Jakabčin. Taking into account thermal residual stresses in topology optimization of structures built by additive manufacturing. *Mathematical Models and Methods in Applied Sciences*, 28(12):2313–2366, 2018.

[5] Grégoire Allaire, François Jouve, and Anca-Maria Toader. Structural optimization using sensitivity analysis and a level-set method. *Journal of Computational Physics*, 194(1):363–393, 2004.

[6] Laura Bittner, Hanno Gottschalk, Michael Gröger, Nadine Moch, Mohamed Saadi, and Sebastian Schmitz. Modeling, minimizing and managing the risk of fatigue for mechanical components. In S. Albeverio, A. Cruzeiro, and D. Holm, editors, *CIB-SGM 2015*, volume 202 of *Springer Proceedings in Mathematics & Statistics*, Cham, 2017. Springer.

[7] Fabien Caubet, Marc Dambrine, Giulio Gargantini, and Jérôme Maynadier. Shape optimization of polynomial functionals under uncertainties on the right-hand side of the state equation. HAL-Preprint, hal-04082741, 2023.

[8] Sergio Conti, Harald Held, Martin Pach, Martin Rumpf, and Rüdiger Schultz. Shape optimization under uncertainty. a stochastic programming perspective. *SIAM Journal on Optimization*, 19(4):1610–1632, 2009.

[9] Marc Dambrine, Charles Dapogny, and Helmut Harbrecht. Shape optimization for quadratic functionals and states with random right-hand sides. *SIAM Journal on Control and Optimization*, 53(5):3081–3103, 2015.

[10] Marc Dambrine, Giulio Gargantini, Helmut Harbrecht, and Jérôme Maynadier. Shape optimization under constraints on the probability of a quadratic functional to exceed a given threshold. *Fachbereich Mathematik, Universität Basel, Switzerland*, Preprint 2023-13, 2023.

[11] Marc Dambrine, Helmut Harbrecht, and Benedicte Puig. Incorporating knowledge on the measurement noise in electrical impedance tomography. *ESAIM: Control, Optimisation and Calculus of Variations*, 25:28, 2019.

[12] Marc Dambrine and Viacheslav Karnaev. Robust obstacle reconstruction in an elastic medium. *Discrete and Continuous Dynamical Systems – B*, 29(1):151–173, 2024.

[13] Charles Dapogny and Florian Feppon. Shape optimization using a level set based mesh evolution method: an overview and tutorial. *Comptes Rendus Mathématique*, 361:1267–1332, 2023.

[14] Frédéric de Gournay. Velocity extension for the level-set method and multiple eigenvalues in shape optimization. *SIAM Journal on Control and Optimization*, 45(1):343–367, 2006.

[15] Michel C. Delfour and Jean-Paul Zolésio. *Shapes and Geometries: Metrics, Analysis, Differential Calculus, and Optimization, Second Edition*. Advances in Design and Control. Society for Industrial and Applied Mathematics, Philadelphia, 2011.

[16] Florian Feppon, Grégoire Allaire, and Charles Dapogny. Null space gradient flows for constrained optimization with applications to shape optimization. *ESAIM: Control, Optimisation and Calculus of Variations*, 26:90, 2020.

[17] Helmut Harbrecht, Michael Peters, and Markus Siebenmorgen. Efficient approximation of random fields for numerical applications. *Numerical Linear Algebra with Applications*, 22(4):596–617, 2015.

[18] Frédéric Hecht. New development in freefem++. *Journal of Numerical Mathematics*, 20(3-4):251–266, 2012.

[19] Antoine Henrot and Michel Pierre. *Shape Variation and Optimization*, volume 28 of *EMS Tracts in Mathematics*. European Mathematical Society (EMS), Zürich, 2018.

[20] M. Loève. *Probability Theory. I+II*. Number 45 in Graduate Texts in Mathematics. Springer, New York, 4th edition, 1977.

[21] Jesús Martínez-Frutos, David Herrero-Pérez, Mathieu Kessler, and Francisco Periago. Risk-averse structural topology optimization under random fields using stochastic expansion methods. *Computer Methods in Applied Mechanics and Engineering*, 330:180–206, 2018.

[22] Bertil Matérn. *Spatial variation*, volume 36 of *Lecture Notes in Statistics*. Springer, Berlin, 2nd edition, 1986.

[23] Stanley Osher and James A. Sethian. Fronts propagating with curvature-dependent speed: Algorithms based on Hamilton-Jacobi formulations. *Journal of Computational Physics*, 79(1):12–49, 1988.

[24] Pavel I. Plotnikov and Jan Sokolowski. Geometric aspects of shape optimization. *The Journal of Geometric Analysis*, 33(7):206, 2023.

[25] Martin H. Sadd. *Elasticity: Theory, Applications, and Numerics*. Academic Press, Burlington, MA, 2nd edition, 2009.

[26] Jan Sokolowski and Jean-Paul Zolésio. *Introduction to Shape Optimization. Shape Sensitivity Analysis*, volume 16 of *Springer Series in Computational Mathematics*. Springer, Berlin-Heidelberg, 1992.

[27] Joseph Wloka. *Partial Differential Equations*. Cambridge University Press, Cambridge, 1987.